THE PERFORMANCE EVALUATION OF A JET FLAP ON AN ADVANCED SUPERSONIC HARRIER

FINAL REPORT

PRINCIPAL INVESTIGATORS

Larry Dean Lipera

Doral R. Sandlin

August 1984

California Polytechnic State University

Aeronautical Engineering Department

San Luis Obispo, California

Grant No. NCC2-238

ABSTRACT

THE PERFORMANCE EVALUATION OF A JET FLAP ON AN ADVANCED SUPERSONIC HARRIER

Larry Dean Lipera

July 1984

The performance of the McDonnell Aircraft Company's concept of a supersonic vertical and short takeoff and landing (V/STOL) fighter, model 279-3, modified to utilize a jet flap has been evaluated. Replacing the rear nozzles of the 279-3 with the jet flap favorably alters the pressure distribution over the airfoil and dramatically increases lift. The result is a significant decrease in takeoff distance, an increase in payload, and an improvement in combat performance.

To investigate the benefit in increased payload, the 279-3 and the jet flapped 279-3JF were modeled on NASA's "Aircraft Synthesis" (ACSYNT) computer code and flown on a 250 ft. takeoff distance interdiction mission. The increase in payload weight that the 279-3JF could carry was converted into fuel in one case, and in another, converted to bomb load. When the fuel was increased, the 279-3JF penetrated into enemy territory almost four times the distance of the 279-3, and therefore increased mission capability. When the bomb load was increased, the 279-3JF carried 14 bombs the same distance the 279-3 carried four. This increase in mission performance and improvements in turning rates was realized with only a small penalty in increased empty weight.

TABLE OF CONTENTS

LIST OF TABLES

LIST OF FIGURES

LIST OF FIGURES

NOMENCLATURE

v	Velocity, ft/s
ρ	Density, slugs/ft^3
s	Wing area, ft^2
AR	Aspect ratio
Q	Dynamic pressure $(\frac{1}{2}\rho v^2)$, $\frac{lbf}{ft^2}$
L	Lift, lbf
W	Weight, lbf
C_D	Drag coefficient $(\frac{Drag}{QS})$
C_L	Lift coefficient $(\frac{L}{QS})$
ΔC_L	Change in lift coefficient
$\Delta C_{L_{max}}$	Change in maximum lift coefficient
$\Delta C'_{L_{max}}$	Change in maximum lift coefficient with full span flaps
C_u	Thrust coefficient $(\frac{Thrust}{QS})$
α_s	Power off stall angle of attack
α_{s_u}	Power on stall angle of attack
$\Delta\alpha_{s_u}$	Change in stall angle of attack due to blowing
δ	Flap angle
$B_o D_o$	Fourier coefficients
t	Time
V_F	Final Velocity
V_i	Initial Velocity
a	Acceleration

NOMENCLATURE

TR	Turning rate, $\frac{\text{degrees}}{\text{sec}}$
g	Gravity (32.2 ft/s^2)
N	Load factor (L/W)
R	Turning radius, ft
ϕ	Bank angle
$\frac{L}{D}$	Lift to drag ratio
Γ	Vortex circulation strength
C_{mac}	Length of mean aerodynamic chord

INTRODUCTION

The propulsive design and integration of aircraft with vertical and short takeoff and landing capability represents an arduous task. So much so that in the case of the early Harriers, Rolls Royce built its Pegasus engine first, and then an airframe was fit around it (the reverse design sequence used on almost all conventional aircraft). This extra effort is justified by the versatility gained by vertical and short takeoff and landing (V/STOL) capability.

V/STOL capability allows aircraft to more successfully complete mission objectives. The AV-8B interdiction mission demonstrates this advantage. The objective of an interdiction mission is to disrupt and/or destroy the opposing forces' logistics. Typical targets include supply bases and roads, petroleum storage, airfields and communications centers. Conventional takeoff and landing aircraft (CTOL) require large runways that are labor and material intensive and therefore are located a considerable distance behind the front lines to ensure their safety. The AV-8B, not needing these elaborate runways, can be stationed very near the front line. The fuel consumed by CTOL aircraft flying to the front line from their remote bases can be converted to payload for V/STOL aircraft such as the AV-8B, and this greater payload can be delivered at a higher frequency. If it is found, upon returning home from such a mission, that the airfield has been bombed, a vertical landing ensures the safety of the pilot and aircraft.

V/STOL air power can also deploy their forces more rapidly, and with a greater survivability. When immediate action is necessary, more V/STOL aircraft can be put into the air in a shorter period of time. These aircraft can also be recovered faster. This is a major advantage for Aircraft Carrier operations. In addition, survivability of the air force is enhanced by the application of multiple basing. If the mother ship is damaged, and unable to serve as an air base, the planes can be offloaded onto smaller ships, or even to portable landing pads on shore.

Because of these advantages, the military has shown an interest in supersonic V/STOL aircraft. The Ames Research Center of NASA is responsible for overseeing the research and development of such concepts, and has issued contracts to various aircraft manufacturers for preliminary design investigations.

One design by the Vought Corporation utilizes a tandem fan engine in which the fan and core turbine are able to operate in parallel and in series. In the parallel mode, each unit has a separate intake, and deflects its exhaust by the use of turning vanes. Rotating the turning vanes redirects the fan air into the engine core for conventional series flow operation.

The General Dynamic E-7 aircraft incorporates ejectors at the wing root to produce vertical thrust. For short field operations the flow from the rear nozzles is diverted into the ejector, which augments the thrust of the engines by entraining the surrounding air into the nozzle flow and thereby increasing the total thrust. Thrust augmentation ratios in excess of 1.5 have been demonstrated using this technique.

Other methods investigated include the use of remote lifting engines operated only during takeoff and landing. One or more lift fans may be used with the possiblity of injecting and igniting fuel in the downstream fan flow for an afterburner effect.

One of the more promising designs that resulted from these studies is the McDonnell Aircraft Company conceptual model 279-3 V/STOL aircraft (Figures 2 and 3). The 279-3 is a single seat, single engine, supersonic fighter/attack aircraft incorporating a very advanced Pegasus engine similar to the engine used in the AV-8B (Figure 1). This engine uses four rotating nozzles to control the direction of the engine's exhaust.

The AV-8B and 279-3, because of their Pegasus engines, are capable of superior maneuvering performance. The engine nozzles can be rotated past ninety degrees, providing rapid deceleration, or the elimination of acceleration in diving flight. In fact, no other aircraft can decelerate more rapidly (50 knots/sec) than the AV-8B. After decelerating, the pilot can accelerate quickly without the time loss associated with engine lag. In addition, judicious application of nozzle rotation can increase the instantaneous turn rate. Very importantly, pilots can perform these maneuvers without giving away their intentions because, unlike airbrake extension, nozzle position is difficult for an opponent to gauge.

As demonstrated in the Falkland Island conflict, the versatility of thrust vectoring makes aircraft with this capability excellent missile platforms. For missiles to be effective, the target must be oriented within a given cone forward of the launching aircraft. The

objective of aerial combat is to position the adversary within the missile's envelope. The thrust vectoring and reaction control system of the AV-8B and 279-3 give them a distinct maneuvering advantage. A rapid deceleration can position a trailing attacking aircraft within the missile's launching envelope. An enemy outside of the missile's launching envelope and forward of the attacking plane can quickly be placed within the envelope by using the reaction control system or independent vectoring to redirect the aircraft. Clearly, the extra maneuverability provided by the Pegasus engine makes the AV-8B and model 279-3 ominous adversaries. It is difficult to win in aerial combat against an adversary that is constantly pointing at you.

The STOL and maneuvering performance of the 279-3 can be increased by using jet flaps. A pure jet flap is a device that allows high pressure air to exit from the trailing edge of the wing at selected angles relative to the freestream flow direction, thereby increasing lift. Although other methods using various blowing techniques (Figure 4) are available for increasing lift, the jet flap was selected for study because it alters the original design of the 279-3 the least, simplifies the performance analysis, and is well suited for such a modification.

Unlike many fighters, the 279-3's engine is located forward, at the root of the wing. Hence, it is a short distance from the engine to the jet flap, which minimizes the length of the duct feeding the flap, reducing pressure losses. Since the rear nozzles that the jet flap replaces are situated at approximately mid-root chord, it is relatively simple to move the ducting, that once provided air to the rear nozzles, into the jet flap.

In previous applications, the jet flap could not produce its maximum lift because of the lack of a system to generate large enough moments to balance the nose down pitching moment created by the jet flap. These nose down pitching moments are generated when the jet flap is deflected, because the center of the lift generated by the blowing is located a significant distance aft of the center of gravity. For the 279-3, the foward nozzles and the Reaction Control System can be used to produce the balancing moments necessary to achieve the maximum lift capability of the jet flap.

The Pegasus engine ingests air through a large fan near the inlet. A portion of this air is directed through the core of the engine with fuel added and burned in the combustion chamber. This core air, along with some by-pass air, is directed through the aft nozzles. Some of the air that passes through the fan is directed through the forward nozzles. Fuel can be injected and ignited in the plenum chamber, and exhausted through these front nozzles for an after-burning effect (referred to as fan stream burning). This arrangement is desirable for the jet flap version of the 279-3 because it avoids the problems caused by passing high pressure, high temperature, after-burned air through the long, thin nozzle of the jet flap. The occurrence of the fuel being burned in the plenum chamber of the front nozzles also generates additional thrust to balance the negative (nose down) jet flap pitching moments.

In this study, the performance of the 279-3 with and without a jet flap will be computed using an aircraft performance code available at the NASA-AMES Research Center, entitled "ACSYNT", and other

theoretical/empirical methods, and compared to other aircraft. The purpose of this study is to demonstrate the benefits gained and penalties paid for the addition of the jet flap. This is accomplished by comparing aircraft takeoff distance, turn rates and radii, and mission performance.

THE MODEL 279-3

McDonnell Aircraft Company (McAir) has used their previous development experience on the AV-8B advanced Harrier in designing the model 279-3, as can be seen in the similarity of their design.

Both the conceptual supersonic 279-3 shown in Figures 2 and 3 (a brief description of the 279-3 geometry and performance is given in Table 1) and the operational AV-8B (Figure 1) utilize a unique engine incorporating four rotating nozzles to provide thrust vectoring. The fan and engine core air are directed through two nozzles forward and two nozzles aft of the center of gravity. In the case of the model 279-3, these two pair of variable area nozzles can be rotated independently through one hundred degrees, measured from the longitudinal axis of the airplane. The 279-3 produces a significantly greater thrust than the AV-8B due to a larger more advanced engine with fan stream burning. Modulation of the fan stream burning with independent vectoring provides pitch control for hovering and low speed flight. Low dynamic pressure, or nozzle rotation, also activates the reaction control system. With this system, thrusters located in the nose, tail, and wing tips, which utilize high pressure air bled from the engines, provide pitching, yawing, and rolling moments.

The horizontal stabilizer for the 279-3 is a canard, located forward of the wing. Since moments created by the wing are negative (nose down), a positive lifting force is required of the canard to balance these moments. This positive lifting force supplements the

lift of the wing. In addition, since the wing is in the wake of the canard, at high angles of attack the canard's vortex interacts with the flow over the wing causing decreased separation and providing an increase in lift and a decrease in drag. These and other aerodynamic and propulsive improvements were made on the 279-3 design, and the result was an agile supersonic V/STOL fighter capable of taking off vertically with heavy loads, and flying at speeds approaching twice the speed of sound.

JET FLAP THEORY

The pure jet flap used on the 279-3JF allows high pressure air to exit from the trailing edge of the flap, producing a long thin jet sheet across a portion of the wing span (Figures 4, 5, and 6). When expelled at angles below the freestream direction, this jet sheet produces an increase in lift that is significantly greater than the lift obtained by thrust vectoring, with no drag increase and only small losses in horizontal thrust.

To understand the method of lift augmentation, an analogy can be made between the mechanical and the jet flap. The mechanical flap increases the camber, and sometimes the chord of the wing, and increases lift when lowered. The jet flap expels a high velocity jet sheet from the wing's trailing edge that is, like the mechanical flap, a boundary between the upper and lower surface flows. This flow boundary favorably alters the pressure distribution on the airfoil. However, the lift produced by a jet flap far exceeds the lift generated by a mechanical flap. D.A. Spence (Reference 1) has related the strength of the jet sheet to a vortex sheet. Joukowski then relates the lift to the circulation through the relation

$$L = \rho v \Gamma$$

Because of this relationship, the extra lift generated by the jet flap is frequently termed super-circulation lift. In addition, directing the high speed air in the jet flap downward creates a further increase

in the vertical lifting force. In fact, lift coefficients of the order of four have been measured with jet flap installations (Reference 2).

Unlike the mechanical flap, no surface exists to transmit forces to the airfoil. Also, the jet flap accelerates the flow in the boundary layer on the wing which tends to delay separation. For these reasons, the jet flap has no skin friction drag or form drag. Therefore, the total drag of the wing with a jet flap is less than that of a mechanical flap.

As shown in Figure 7, the freestream flow field turns the jet sheet in the direction of flight. For inviscid flow, if the control volume is drawn large enough, you can conclude, using momentum theory, that the change in momentum is independent of the deflection angle. This is referred to as thrust recovery. However, viscosity causes mixing of the jet sheet with the external flow and results in momentum losses. Also, at large deflection angles and blowing coefficients, a separation bubble is created at the wings leading edge as explained in Reference 3. This separation causes a large reduction in thrust recovery, above that caused by the jet mixing. At small jet flap angles, the momentum change is only slightly dependent on deflection angle and, therefore, only small losses in horizontal thrust can be expected. This is true only for high aspect ratio nozzles which expel a long thin sheet of air. The low aspect ratio nozzles of the AV-8B and 279-3 experience negligible thrust recovery. Thus, the jet flap has the ability to increase lift dramatically with no drag penalty and very little thrust loss.

THE JET FLAPPED 279-3

The design principle followed in adding the jet flap to the 279-3 was to minimize the configuration changes. Aerodynamic data exists for the 279-3 and can be used for the 279-3JF if the shapes of the two vehicles are essentially the same.

As shown in Figures 5 and 6, the flap exhaust area spans about one quarter of the wing, or the inner half of the existing flap. This exhaust region is a compromise between various design considerations. A long nozzle, blowing a large portion of the wing span increases the jet flap lift, but adds structural weight necessary to support the flap. The 17 aspect ratio nozzle (length divided by width) used in Reference 4 is a reasonable compromise between the above constraints, and was used on the 279-3. Keeping the exit area of the jet flap equal to the maximum exit area of the nozzle it replaced, resulted in a nozzle length of 4.5 feet and thickness of 3.1 inches. This nozzle was found to be so effective that not all of the extra lift could be utilized for increased payload and still stay below the maximum weight imposed on the airframe. Therefore, no further advantage would be gained by using a higher aspect ratio nozzle.

The large jet flap deflection angles and high speed airflow through the flap can cause leading edge separation. For this reason, the leading edge flaps were replaced with the more effective slats (no weight penalty assessed). The addition of the slats and the jet flap, and the elimination of the rear nozzles, were the only alterations

made to the 279-3. The manufacturer's published aerodynamic data for the 279-3 was then used for the 279-3JF, since the geometry of the two aircraft are essentially the same.

PROCEDURE

Takeoff Performance

Since one advantage of the model 279-3 is its ability to take-off in short distances carrying heavy loads, it is useful to evaluate the change in the performance resulting from the addition of the jet flap. To do this, lift, drag, thrust, and weight penalties or benefits of the jet flap must be estimated and superimposed on the known characteristics of the 279-3, given in Reference 5.

Minimum takeoff distance is accomplished by rotating the 279-3JF to its maximum lift coefficient, while simultaneously rotating the engine nozzles to predetermined angles, as soon as the aerodynamic lift and vertical thrust equals the weight of the aircraft. Estimating maximum lift coefficients is difficult because not all of the lift that can be produced by a high lift device is necessarily usable lift. The particular lifting characteristics and geometry of the wing, and the jet flap size and location must be considered. For example, theory might predict that tenfold increases in lift can be achieved with a jet flap, but in reality the wing would stall long before reaching such large lift coefficients. The methods of David J. Moorhouse (References 6 and 7) were used to estimate the maximum lift of the jet flapped 279-3, and take into account not only the design of the jet flap, but also the wing planform that it is installed on. In his reports, David J. Moorhouse shows excellent correlation of his results with empirical data. His methods are applicable to wing aspect ratios

"greater than approximately three,"[6] and independent of sweep angle. The aspect ratio of the 279-3 is exactly three. Furthermore, he estimates the stalling characteristics of the jet flapped wing. Using Moorhouse's methods, the change in the maximum lift coefficient is given by

$$\Delta C_{L_{max}} = K_b \left[\Delta C'_{L_{max}} - C_u \sin (\alpha_{s_u} + \delta) \right] + C_u \sin (\alpha_{s_u} + \delta) \qquad \text{Eq. 1}$$

where,

$$\Delta C'_{L_{max}} = 5.5\pi \left[\frac{B_o \alpha_{s_u} + D_o \delta}{1 + \frac{B_o}{2}} \right] \left[\frac{AR + .637 C_u}{AR + 2 + .604\sqrt{C_u} + .876 C_u} \right] \qquad \text{Eq. 2}$$

$\Delta C'_{L_{max}}$ is the change in the maximum lift coefficient for a full span flap, and the terms containing the trigonometric sine are the lift component of the jet flap's vertical thrust. The variable K_b in equation 1 takes into account the partial span of the jet flaps. In this design, with 0.246 of the wing span being blown, Moorhouse assumes K_b to be the constant 0.35. C_u is the thrust coefficient and is the ratio of the gross thrust of the jet flap to the dynamic pressure of the freestream times the wing area. A large thrust coefficient indicates a prominent jet sheet, projecting far into the freestream. α_{s_u} is the power on stall angle of attack and δ is the jet flap deflection angle. The term "power on" refers to conditions when the jet flap is operating. Power off conditions are without any blowing, and thus refer to the baseline 279-3. B_o and D_o are Fourier coefficients given graphically in Reference 6, and are functions of the thrust coefficient. Since graphical representations cannot be conveniently used in computer

programs, mathematical expressions were developed to represent B_o and D_o. These mathematical expressions are given by,

$$B_o = .185\ C_u^{0.833} \qquad \text{Eq. 3}$$

$$D_o = .3204\ C_u^{0.6374} \qquad \text{Eq. 4}$$

shown in Figures 8 and 9. The relationship between α_{s_u} and α_s (the power off stall angle) is given by

$$\alpha_{s_u} = \alpha_s + \Delta\alpha_{s_u} \qquad \text{Eq. 5}$$

$$\Delta\alpha_{s_u} = -\frac{1}{2}\left[\frac{B_o\alpha + D_o\delta}{1 + \frac{B_o}{2}}\right] \qquad \text{Eq. 6}$$

The negative sign in equation 6 indicates that there is a decrease in the stall angle of attack, which also occurs when a mechanical flap is deflected.

The only unknown in the above equation, given the flap angle and the aircraft velocity and gross thrust needed to determine the thrust coefficient, is α_s of the baseline 279-3. In addition, equation 1 does not predict the maximum lift coefficient, only its change due to the jet flap. Thus, $C_{L_{max}}$ of the baseline 279-3 must also be determined and added to equation 1. The values of α_s and $C_{L_{max}}$ of the baseline 279-3, are determined from information given in Reference 5, and are functions of the mechanical flap deflection. Values of $C_{L_{max}}$ and α_s for various deflection angles (δ) were taken from Reference 5, curves were fit (see Figures 10 and 11), and the equations below were generated to represent the curves.

$$\alpha_s = -0.2501\delta + 0.5585 \qquad \text{Eq. 7}$$

$$C_{L_{max}} = \frac{\delta + 4.0384}{2.4929} \quad (\delta \text{ in radians}) \qquad \text{Eq. 8}$$

Thus, $C_{L_{max}}$ given by equation 8 is added to $\Delta C_{L_{max}}$ (equation 1) to determine the total wing lift and vertical thrust of the jet flap. Adding this to the vertical thrust component of the front nozzles, the maximum lift and therefore the maximum takeoff weight is obtained.

At the lift off point, there must be enough thrust to overcome drag and provide an acceleration. Thus, the drag of the aircraft at maximum lift must be determined. It was assumed that the drag of the 279-3JF at $C_{L_{max}}$ was equal to that of the 279-3. As explained previously, the jet sheet cannot transmit a drag force to the airfoil. In addition, the jet flap attains its maximum lift at much smaller angles of attack than the unblown wing, and the 279-3JF does not experience the parasite drag of the rear nozzles since they were eliminated. Thus, the assumption of equivalent drag at $C_{L_{max}}$ for both aircraft is conservative. Values of drag at $C_{L_{max}}$ were obtained from information contained in Reference 5. This data was also curve fitted (Figure 12) and the equation of this curve was found to be

$$C_D = 0.461 + 0.265\sqrt{\sin\delta} \quad (\delta \text{ in radians}) \qquad \text{Eq. 9}$$

Equations 7, 8, and 9 are used in the computer program given in Figure 13 to determine the lift and drag at lift off, for various flap deflections.

Thrust recovery, as applied to jet flaps, refers to the ability of the jet flap to recover a large portion of the engine's thrust as a forward propelling force, even though the nozzles exhaust is directed at angles to the freestream. Recovery of almost all the total thrust is possible at small thrust coefficients, or small deflection angles. However, the low takeoff speeds of the 279-3JF produce large thrust coefficients, and the maximum lift benefit can be achieved only at large deflection angles. Because of this, the thrust recovery is limited during takeoff, and only the trigonometric cosine of the deflection angle multiplied by the total thrust was used to propel the aircraft forward (i.e., zero thrust recovery).

The performance of the 17 aspect ratio nozzle was assumed to be equal to the axisymmetric nozzle that it replaced. This assumption is supported by Reference 4, where a performance comparison was made between a 17 aspect ratio ADEN nozzle and a conventional axisymmetric nozzle. Taking into account leakage and pressure drop effects, the 17 aspect ratio nozzle was found to be comparable in performance. The 17 aspect ratio nozzle studied in Reference 4 had afterburners located inside the nozzle, which resulted in thrust losses when they were not in use. The 279-3JF does not have an afterburner in the jet flap nozzle, and therefore doesn't experience these thrust losses.

No thrust penalties were assessed to the 279-3JF due to the added length of ducting required to divert the engine flow into the jet flap. Even if these losses were considered, they would be relatively small because the rear nozzles of the 279-3 are already very near the proposed location of the jet flap, which minimizes duct

length and hence thrust losses. The engine performance of the 279-3, which is also applied to the 279-3JF, was developed by Reference 8 (see Appendix A).

Although it is assumed that there is no thrust loss incurred by using the 17 aspect ratio nozzle, there is a weight penalty. Reference 4 estimates the 17 aspect ratio nozzle, with burner and other required hardware, to weigh 488 lbf more than the axisymmetric nozzle. In the case of the 279-3JF, the engine fan air flowing through the forward nozzles is burned. Since the core air flowing through the jet flap is not burned, the weight of the afterburner can be subtracted. The afterburner weight of an engine of similar size as the advanced Pegasus engine has been determined to be 184 lbf. The additional weight of the 279-3JF over the baseline 279-3 is then 304 lbf. The bulk of this added mass is primarily the result of added internal wing structure to contain the high pressure exhaust flow. This 304 lbf weight penalty is used in all performance calculations.

The additional lift, drag, thrust and weight of the 279-3JF are determined, and included to predict takeoff performance. This was accomplished by developing a computer code which included all of the applicable terms, and is shown in Figure 13. Given the takeoff velocity, this program calculates the maximum takeoff weight and the takeoff distance required to reach the given takeoff velocity. The methods previously described were used to estimate the maximum lift coefficient. However not all the lift computed in this manner is necessarily usable lift. The aircraft must be balanced, the stall angle must be above the selected value of five degrees, and the

nozzles must not be rotated so far forward that there is insufficient thrust for acceleration. In generating the takeoff data, equivalent short takeoff techniques used by McAir for the 279-3 were used. The nozzles were positioned to ten degrees below horizontal until lift-off, and then were rotated to an angle which resulted in the lift being equal to the weight, with the logitudinal acceleration not allowed below 0.065g.

To determine the maximum balanced lift achievable, the front nozzles were rotated to the vertical, with maximum thrust including burning, supplying their greatest positive pitching moment. The rear nozzles were rotated to the maximum deflection angle that would balance the moments produced by the front nozzles. The moments produced by the jet flap resulted from aerodynamic lift, which was assumed to act at the midpoint of the mean aerodynamic chord (Reference 1), the weight of the jet flap, and its vertical thrust component. Both the added weight and vertical thrust acted on the flap hinge line. The configuration was assumed neutrally stable, with the center of gravity and aerodynamic center at the quarter chord position of the mean aerodynamic chord. A free body diagram depicting the forces involved in the balancing criteria is given in Figure 14. Note that due to the low takeoff speeds, and lack of data, the canard (or reaction control system) was not used for trimming. In practice, any canard lift would supplement the moments created by the front nozzles. This would permit the rear nozzles to be deflected further, allowing a greater lift to be generated.

With the front and rear nozzles' positions set by the balancing criteria, further adjustments might still have to be made. The jet flap, like the mechanical flap, increases the maximum lift of the aircraft. However, the angle of attack at which the maximum lift coefficient is attained is decreased. Because jet flaps are a much more powerful device than a mechanical flap, the decrease in stall angle is much greater. This is the reason why powerful leading edge devices are needed, such as the slats used on the 279-3JF. Slats were assumed to increase the stall angle by ten degrees (Reference 6). Considering this, the minimum stall angle was set at five degrees for the 279-3JF. If the stall angle was below five degrees, the rear nozzles were rotated up, decreasing the lift, and increasing the stall angle.

In addition to the stall angle restriction, the longitudinal acceleration of the aircraft at lift-off could not be below 0.065g. Acceleration provides a build up of speed, necessary to increase lift above the weight so the aircraft will climb. The front nozzles are vertical for balance and lift and, therefore, provide no horizontal thrust to overcome drag. The large rear nozzle deflection provides lift, but also limits the horizontal thrust component and increases drag. If not enough horizontal thrust is provided by the rear nozzles, the front nozzles must be rotated aft. Although rotating the front nozzles away from the vertical decreases the lifting force, and pitching moment, it is still more desirable to use the front nozzles to provide sufficient acceleration than the rear nozzles. Rotating the rear nozzles aft significantly decreases the jet flap lift, which is a strong function of deflection angle.

Once the lift is determined that satisfies the balancing condition, the stall angle restriction and the acceleration requirement, the takeoff distance required to accelerate to the takeoff velocity can be determined. If the initial velocity (V_i), the final velocity (V_F), and the acceleration (a) of a vehicle are known, the time (t) required to reach the terminal velocity can be determined from the simple physics equation

$$t = \frac{V_f - V_i}{a}$$

The distance covered in this time interval can then be computed by multiplying the time by the average velocity. The only unknown is the aircraft's acceleration, which can be determined from Newton's Law. The net force used is the thrust of the engine minus the drag of the aircraft. The engine was assumed to produce its maximum sea level static thrust throughout the entire takeoff. Because of the low takeoff velocities, and thus negligible ram drag, this introduced little error. Since the total drag of the aircraft varies with the square of the velocity, and the velocity is varying, additional small errors were introduced by evaluating the drag at a constant velocity.

The total takeoff distance, from a zero initial velocity to the takeoff velocity is divided into ten intervals. The acceleration, time, and distance covered in each interval is computed and the total takeoff distance is equal to the sum of all the distances covered in each interval. For example, if the takeoff weight and distance is desired for a takeoff velocity of 100 ft/s, the computer program first

determines the maximum usable lift that can be obtained at this speed. Then the takeoff distance is broken into ten velocity segments, each equal to 10 ft/s. The takeoff distance necessary to reach 10 ft/s from a stationary position is computed, then the distance required to reach 20 ft/s from 10 ft/s is determined, and this process is repeated for each of the ten intervals. The total takeoff distance is the sum of the distances computed in each of the intervals.

Maneuvering Performance

The lift augmentation provided by the jet flap not only benefits takeoff performance but also improves turning rates. Maximum instantaneous turning rates are directly proportional to maximum lift coefficients obtainable, and are limited by the structural design of the aircraft. Since high angles of attack are usually produced in performing tight turning maneuvers, a component of the engine thrust that is equal to the sine of the angle of attack will be added to increase total lift. Therefore, all aircraft are capable of increased turning rates due to this effect, which is considerable at high angle of attack. The model 279-3, capable of rotating its thrust direction past ninety degrees, can place its total thrusting force parallel to the direction of lift, greatly improving instantaneous turning rates. In addition to the thrust vectoring benefit, the 279-3JF produces higher $C_{L_{max}}$ values due to the jet flap effect, which further increases turning rates.

In computing the 279-3JF's maximum instantaneous turn rates, the nozzles were rotated to an angle of ninety degrees (relative to

the fuselage centerline) minus the stall angle of attack. This placed the gross thrust in the direction of lift. The Moorhouse relations for the change in the maximum lift coefficient at this jet flap deflection angle was added to the maximum lift coefficient of the 279-3 to determine the aerodynamic lift. The aerodynamic lift and the gross thrust of the engine were combined to determine total lift. With the flight speed and aircraft weight known, the turning rates and radii were computed by using the equations shown below.

$$TR = \frac{g}{V} \cdot \sqrt{N^2 - 1} \qquad \text{Eq. 10}$$

$$R = \frac{V^2}{g \tan \phi} \qquad \text{Eq. 11}$$

Note that instantaneous turning rate (TR) and radius (R) are independent of drag. No jet flap thrust penalties were assessed. These equations were incorporated into a computer program to compute turning rates and radii of the 279-3JF at various altitudes and speeds. The program given in Figure 15 computes desired values for a Mach number of 0.4, and an altitude of 10,000 ft. In order to compare the turning performance of the 279-3 and 279-3JF, an aircraft weight of 26,260 lbf was used, consistant with Reference 5. For the 279-3JF, 304 lbf of the aircraft weight consisted of the jet flap.

Mission Performance

The jet flapped 279-3JF can takeoff, in a given distance, at a much greater takeoff weight than the 279-3. This extra weight

translates directly into a greater payload. How much more useable payload, and its effects on mission performance was determined by computer modeling the 279-3 and 279-3JF, using the ACSYNT Program, and comparing the results obtained from numerous computer runs.

ACSYNT is the NASA Ames conceptual/preliminary design FORTRAN program for Aircraft Synthesis. This program predicts the mission performance (fuel consumption, climb rates, cruise conditions, etc.) of an aircraft within five percent. ACSYNT is divided into numerous modules, or subprograms, each capable of the analysis of a specific aircraft characteristic. For example, in the aerodynamics module, the lift and drag characteristics are determined. For an accurate model, this module was adjusted to predict the aerodynamics of the 279-3 given in Reference 5. The detailed weight statements required by the weight module are also given in Reference 5. The propulsion module must accurately predict the characteristics of the engine over its entire operating cycle. Engine data was generated by Charles L. Zola of NASA-Lewis, listed in Reference 8, using a Pratt and Whitney cycle analysis code. This data was input into ACSYNT's engine module. Once all of ACSYNT's modules are supplied with the correct data, the computer program accurately predicts the performance of the aircraft that is modeled. The modeled 279-3 is discussed in Appendix A. Due to similar geometry, the 279-3 and 279-3JF have the same aerodynamic characteristics, and no jet flap lift benefit was given to 279-3JF in cruise or climbing flight. The only difference between the data for the 279-3 and 279-3JF was the 304 lbf weight of the jet flap.

Once modeled, each aircraft was run on a common mission, and the performance compared. The mission was a 250 ft takeoff distance interdiction mission shown in Figure 16. This STO mission is typical for V/STOL aircraft, and demonstrates the overwhelming advantage of the jet flap. The 279-3 was "flown" on this mission and its radius, weapons load and other parameters were determined. The 279-3JF was "flown" on this interdiction mission twice, once with the extra payload converted to fuel, and again with the extra weight converted to bombs and fuel. In the first mission, the increase in the mission radius over the 279-3 was determined. In the second mission, enough fuel was added to keep the radius equivalent to the 279-3's radius, but with the weight benefit used to increase bomb load. The configurations of the two aircraft for these missions is shown in Figures 17, 18 and 19.

RESULTS AND DISCUSSION

Takeoff Performance

The program given in Figure 13 was used to generate takeoff performance of the 279-3JF. The takeoff weight versus takeoff distance is compared for the 279-3 and 279-3JF in Figure 20, and demonstrates that the jet flap enables the 279-3JF to takeoff in a much shorter distance for a given weight. At a weight of 54,000 lbf, the 279-3JF takes almost 1,000 feet less distance to become airborn, a decrease by a factor of six. In actual operation, a given distance might be required for takeoff, such as the deck length of a ship. In this case the curves in Figure 20 show that for a fixed takeoff distance, the 279-3JF can carry a considerable increase in payload. The benefits of the increased payload are discussed in the following "mission performance" section.

Table 2 gives a more detailed output of the takeoff performance generated by the compter code. Note that the aerodynamic lift coefficient increase of the jet flap given in this table does not include the vertical thrust of the jet flap nozzles. This data reveals that the rear nozzle angle is 41.3 degrees at 60 ft/s lift off velocity, increases to 69.3 degrees at 110 ft/s, then decreases at higher velocities. It is important to understand why the rear nozzles were not rotated beyond these values.

The small jet flap deflection angle is due to the large thrust coefficient at low dynamic pressures. Since the stall angle is a function of the thrust coefficient, the aircraft stalls at low angles

of attack. Thus, the rear nozzle rotation is kept small to satisfy the stall angle criterion. At velocities higher than 110 ft/s, much larger lift forces can be generated. However, the front nozzles can not balance the large pitching moment produced by the lift. If the lift of the canard was not neglected as was done here, it could aid the front nozzles in countering the pitching moment of the jet flap, and a greater lift benefit could be obtained. Thus, the jet flap was limited in its range by the stall angle at low takeoff velocities, and the balancing conditions at higher velocities.

Combat Performance

Figure 15 shows the FORTRAN code used to compute the instantaneous turning rate and radius of the 279-3JF at an altitude of 10,000 ft and Mach 0.4. By inputing different values of velocity, density, thrust, and $C_{L_{max}}$ into this program, the maneuvering performance at various Mach numbers was determined. It was assumed that the pitching moments created by the jet flap could be balanced by the canard and front nozzles.

The maneuvering performance of the 279-3 and 279-3JF are compared in Table 3. The maximum power-off lift coefficients for the 279-3 are given in Reference 5. The increase in maximum lift due to the jet flap was then added to these values to determine the total lift of the 279-3JF. The power-off lift coefficients given in Reference 5 were generated by deflecting the mechanical flaps. Deflection of the mechanical flaps not only produce a greater lift on the wing, but also creates a nose down pitching moment. To balance the aircraft,

this moment is countered by canard surface lift. The extra lift of the wing and canard increases the maximum instantaneous turning rates. However, the values of $C_{L_{max}}$ used by McAir were not based on balancing the aircraft by deflecting the trailing edge flaps. For this reason, the performance given in Table 3 for the 279-3 is conservative. Even though the two aircraft are balanced differently, an interesting comparison can be made.

At 10,000 ft and Mach 0.4, the aerodynamic lift coefficient of the jet flapped fighter is 2.27. The maximum lift coefficient of the 279-3, even if the trailing edge flaps were deflected, is only 1.9. At the above altitude and flight speed, the 279-3JF would then generate over 25,800 lbf more lift than the 279-3, which is equivalent to a turning rate advantage of 4.3 degrees per second.

Increases in maximum sustained turning rates are also obtained. In a maximum sustained turn, the pilot increases lift until the drag of the aircraft (a function of lift) equals the thrust in the direction of flight. With thrust equal to drag, the turn can be sustained indefinitely, and the lift at the sustained condition determines the turning rate.

Examination of Equations 1 and 2, which govern jet flap lift reveals that an increase in maximum lift is realized even at a zero flap deflection angle. This lift benefit is also realized at all angles of attack, which permits sustained turning rates to be determined.

At 30,000 ft and Mach 0.6, $\Delta C_{L_{max}}$ is 0.033 with no flap deflection. This extra lift corresponds to 2,267 lbf, and increases the

sustained turning rate. Small flap deflections would further increase the lift, while total forward thrust would be maintained through thrust recovery. However, there would be an increase in drag due to the mechanical flap deflection, which could result in a loss in performance.

In order to compare the 279-3JF to current aircraft, Table 4 is presented with instantaneous turning rates given for the 279-3JF and for other American and Soviet built fighters (Reference 9). This comparison shows that the maneuvering performance of the 279-3JF is far superior to present day, state-of-the-art fighters.

Mission Performance

It has been demonstrated that the 279-3JF can takeoff, in a given distance, with a greater payload than the 279-3. How much more useable payload, and its effects on mission performance is determined by modeling each aircraft and comparing their ACSYNT predicted performance on a typical mission. The mission selected was a 250 ft STO interdiction mission depicted in Figure 16. The takeoff distance of 250 ft limited the 279-3 to a weight of 42,000 lbf (Figure 20). The 279-3JF, however, can takeoff in the same distance weighing over 56,000 lbf. Because McAir published their takeoff results only up to a gross weight of 54,000 lbf, this limit was also applied to the 279-3JF. At this weight, the 279-3JF's adjusted takeoff distance is only 211 feet (Figure 20). The extra 12,000 lbf (304 lbf of which is the jet flap) was then added to the jet flapped model in two forms. In one mission the extra payload was converted to fuel, and the increase in mission

radius was determined. In another, the payload was converted to bombs, and enough fuel was added to keep its radius comparable to that flown by the 279-3. The configuration and performance of the 279-3 and 279-3JF on the interdiction mission are given in Figures 17, 18 and 19.

The 279-3JF is clearly the more effective aircraft. Carrying the same number of bombs and missiles, it penetrated 564 miles behind enemy lines, compared to 152 miles for the 279-3. This is an increase in mission radius by almost a factor of four. Keeping the mission radius approximately the same by increasing the number of bombs and the amount of fuel, the 279-3JF delivered fourteen MK-82 bombs to the same target that the 279-3 could deliver only four. Thus, with 39 feet less takeoff distance, the jet flapped 279-3JF increased the mission capability by either reaching enemy positions that the 279-3 could not, or by carrying ten more bombs to a common target.

It should be noted that the mission performance of the 279-3JF is conservative because equal lift to drag ratios (L/D) were assumed for both aircraft. In practice, the jet flap increases the L/D, which is a measure of aerodynamic efficiency. As shown in the turning performance section, the jet flap increases lift even with no flap deflection. At the cruise conditions for the comparison mission (Mach 0.9, 41,000 ft), the jet flap adds 1,738 lbf more lift. Knowing the lift and drag of the 279-3 (given by ACSYNT), the L/D for the 279-3JF was determined to be 7.36 at zero flap deflection. ACSYNT predicted the L/D of the 279-3 to be 7.11. The 279-3JF is therefore more aerodynamically efficient and its performance is greater than predicted.

Additional Jet Flap Benefits

Although no data was obtained, the jet flap has additional advantages. The jet flap also reduces the infrared (IR) signature, which is a measure of thermal radiation. An aircraft with a large IR signature is easily revealed to enemy forces, and can be shot down by heat (IR) seeking missiles. The 279-3 already has a reduced IR signature because the hot engine components are shielded by the angled nozzles. The jet flap has the potential to suppress the IR signature further, due to the large exposed surface area of the jet sheet. Since heat transfer is directly proportional to surface area, large heat transfer to the cooler ambient air can be expected, reducing the temperatures, and thus the IR signature.

Another consideration is the effects of the jet on ground crew and landing pads during takeoff and landing. The high temperature and velocity of the jet can hinder ground crew operations and quickly destroy landing surfaces. The severity of these effects would be reduced with the cooler, less concentrated jet sheet.

CONCLUSION

The purpose of this study was to evaluate the benefits and penalties for the addition of a jet flap on the advanced supersonic Harrier model 279-3. The jet flap is a device that expels a long thin sheet of air along the span of the wing, increasing lift. The jet flapped 279-3JF was compared to the 279-3 on the basis of takeoff performance, maneuvering performance and mission performance. The conclusions drawn from these comparisons are as follows:

1. The jet flap enabled the aircraft to takeoff in a much shorter distance for the same weight, or in the same distance, but carrying a greater payload.
2. The lift benefit of the jet flap increased instantaneous turning rates and decreased turning radii. Similar improvements in sustained turning rates and radii can be expected.
3. Mission performance was increased. On a 250 ft interdiction mission, the 279-3JF could either deliver more bombs to the same target as the 279-3, or deliver the same number of bombs to a target that is out of the 279-3's range.
4. The infrared signature is reduced.
5. Landing pad wear is reduced, and a safer environment is provided for the ground crew.

It has been shown that there is a lot to gain by adding a jet flap to the 279-3. However, in order to realize the jet flap's fullest

potential, the entire aircraft should be designed around the jet flap, instead of merely adding it onto the existing design. Three considerations demonstrate this point.

First, the sizing of the aircraft should be reassessed. In this design, all the added lift could not be utilized as payload, because the gross takeoff weight, a structural limitation, would be exceeded. This indicates that the engine and airframe are not properly matched. Reducing the size of the engine would maintain the original performance of the 279-3, while decreasing fuel consumption. Also, enlarging the airframe would properly match the airframe to the engine. A design study should be made to select the best possible method to resize the aircraft.

Second, the jet flap increases lift even at zero deflection angle. In cruise, the added lift creates moments that must be countered by control surface deflections. Since surface deflections produce drag, this trim drag can cause a significant loss in aerodynamic efficiency. With judicial wing/canard placement and by redistributing the weight, this trim drag could be reduced.

Although the 279-3JF clearly demonstrates the tremendous advantage of the jet flap, its full potential could not be realized. Even though independent vectoring of the front nozzles provide large positive moments necessary to balance the aircraft, the jet flap rotation was still limited at high velocities because of the balancing conditions. This suggests that a better design would be a tandem wing aircraft, with jet flaps located on both wings. Each jet flap could then be used to its fullest potential with the moments created on each wing

balanced by the other. This again points out the importance of the airframe/jet flap match, and the need to develop the aircraft around the jet flap.

The final decision on whether to incorporate a jet flap into a design should be based on the trade offs involved. The added versatility is gained with only a slight weight penalty and (although not considered in this study) a thrust loss. However, the extent of this added versatility must be examined. If STOL performance is not required the jet flap would lose some of its advantage. Also, since the jet flap increases aerodynamic lift, and therefore requires a flow about the wing, no lift benefit would be realized for vertical takeoffs. Thus, the decision to incorporate jet flaps into a design should be based on whether the increase in versatility justifies the added complexity and cost.

APPENDIX A

FIGURES AND TABLES

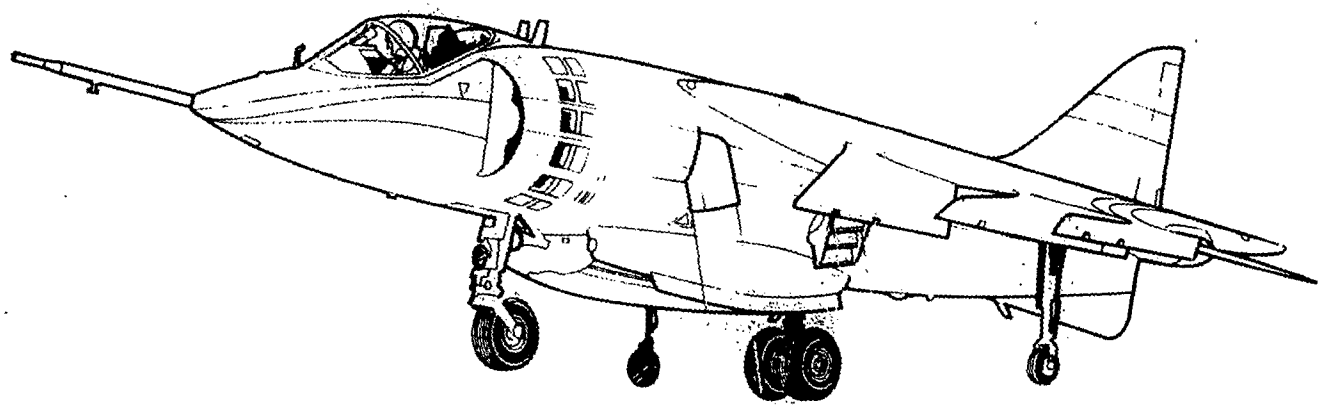

FIGURE 1- AV-8B Harrier

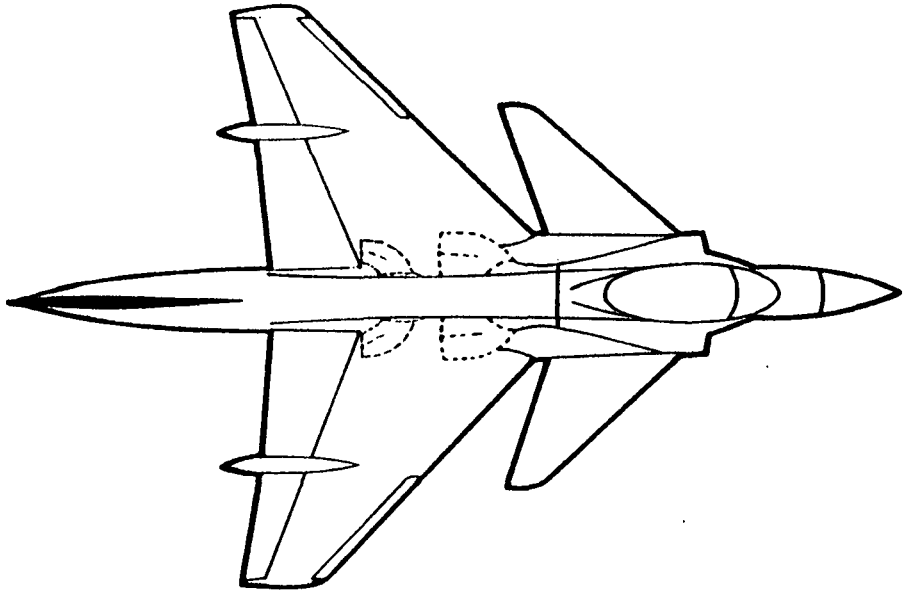

FIGURE 2-Top View of Model 279-3
(from Reference 5)

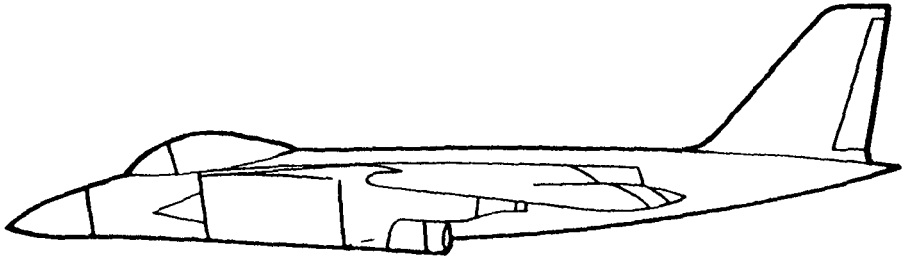

FIGURE 3- Side View of Model 279-3
(from Reference 5)

TABLE 1

SUMMARY OF AIRPLANE CHARACTERISTICS

279-3

Wing	
Area	428.4 ft^2
Aspect Ratio	3.0
Taper Ratio	0.25
Leading Edge Sweep	45°
Vertical Tail	
Area	65.0 ft^2
Fuselage	
Length	56.0 ft
Canard	
Area	85.6 ft
Weights (in lbf)	
Maximum Gross (250 ft STO)	42,000
Maximum Gross (VTO)	29,840
Empty	18,827
Internal Fuel	10,061
Propulsion System	4,415
Thrust	
Maximum Afterburning (sea level static, standard day)	38,420 lbf

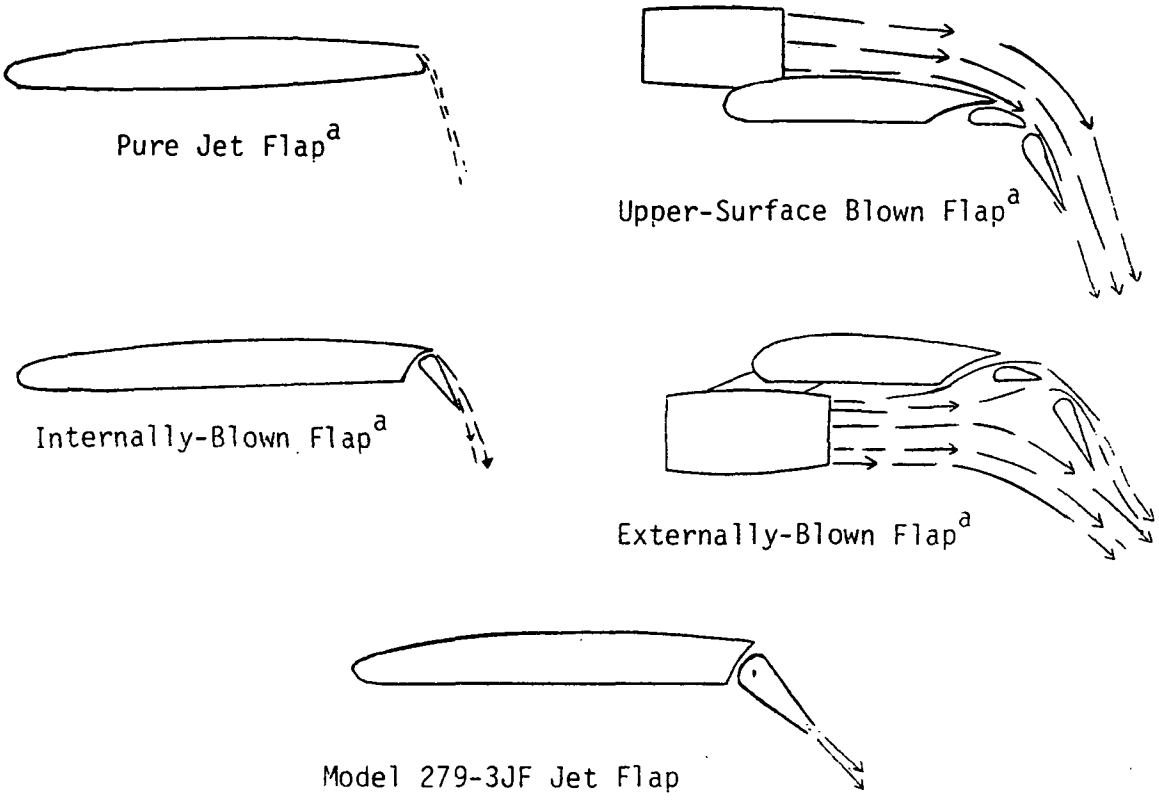

[a]Reference 6

FIGURE 4- Powered Flap Concepts

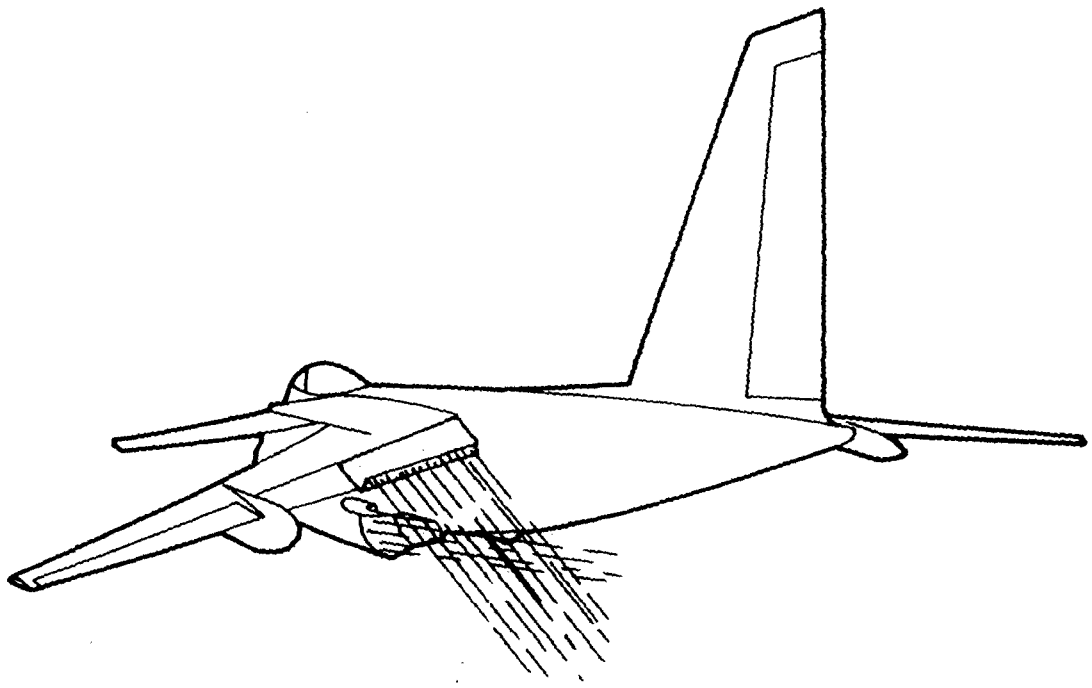

FIGURE 5- model 279-3JF

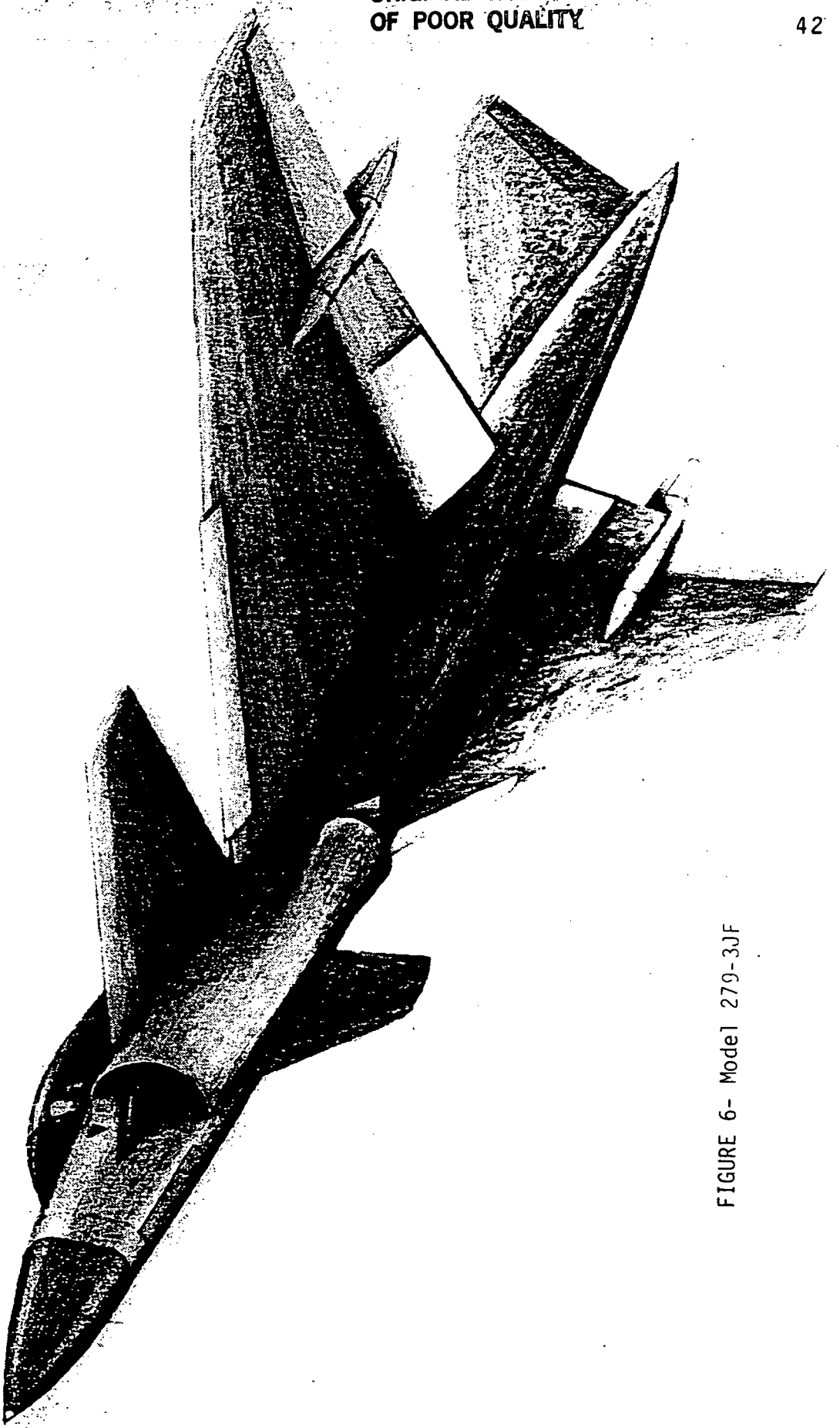

FIGURE 6- Model 279-3JF

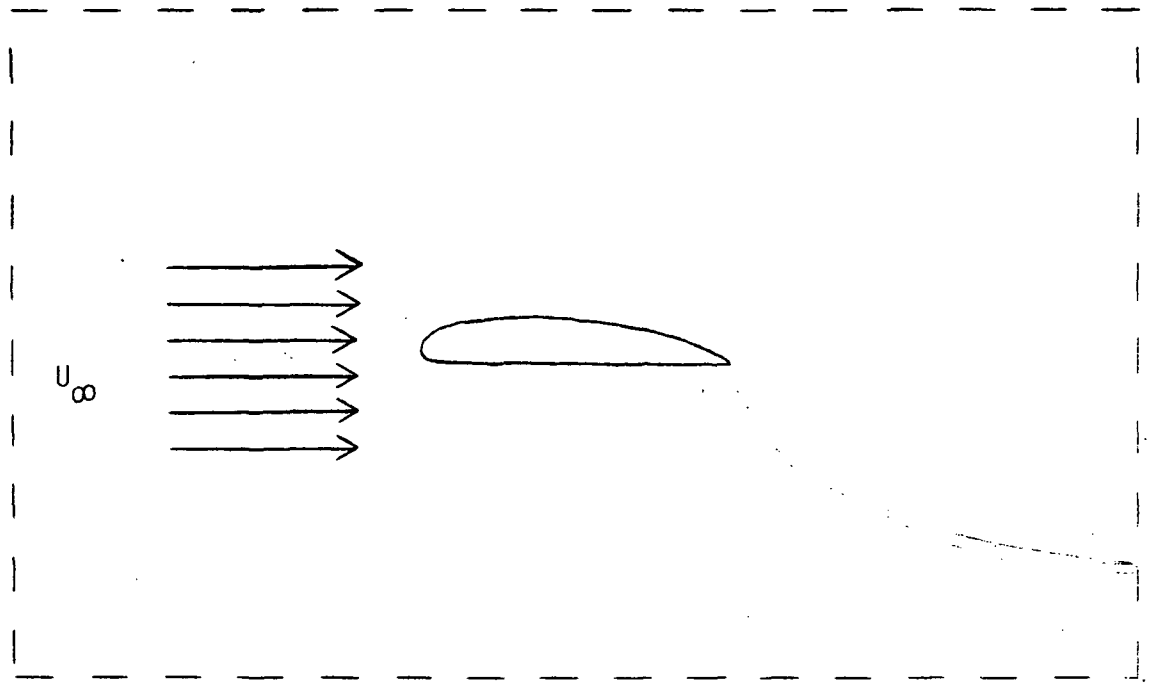

Jet Sheet being turned by, and parallel to, the freestream flow

FIGURE 7 (from Reference 3)

Method of Thrust Recovery

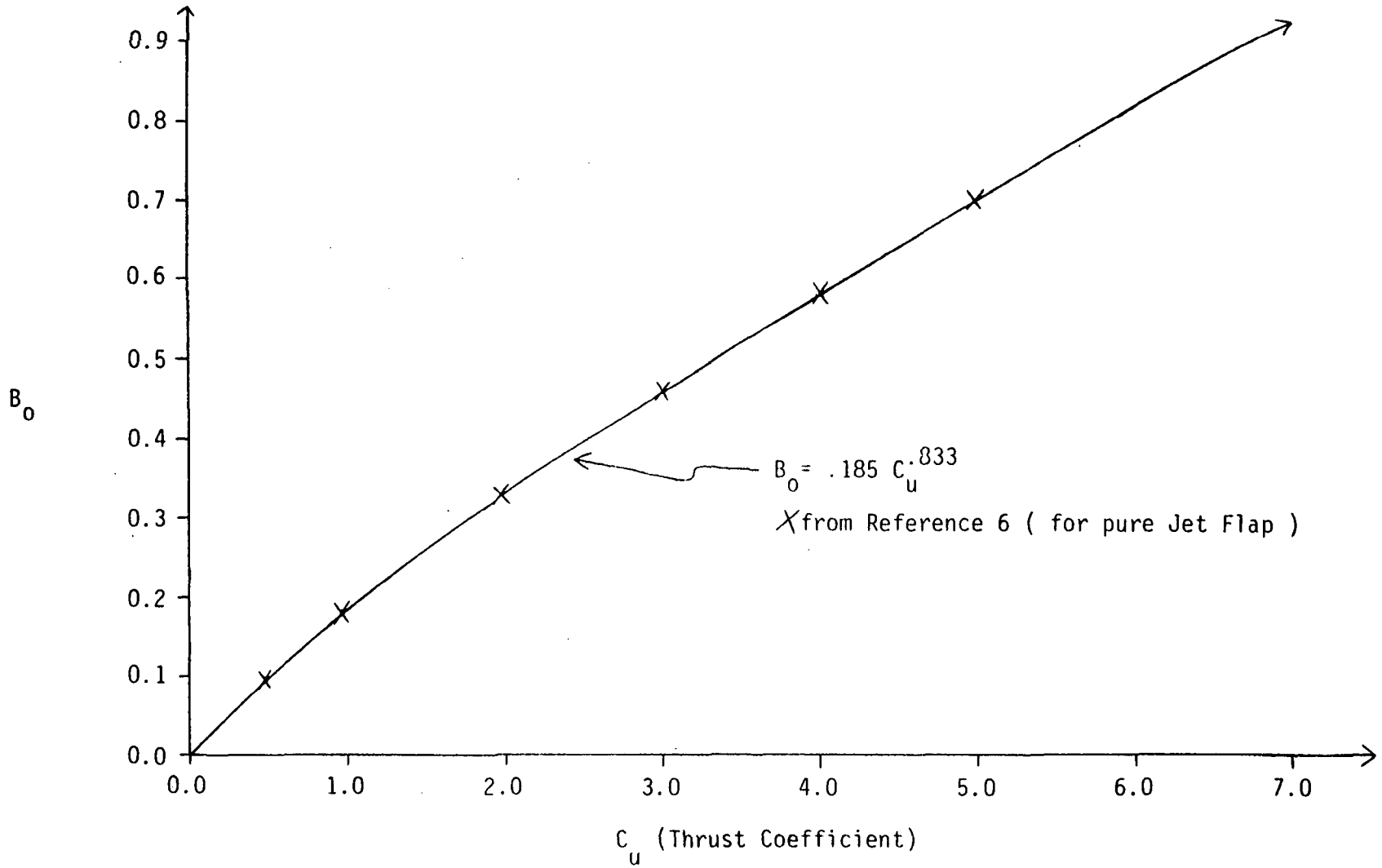

FIGURE 8- Curve of Fourier Coefficient B_o Versus Thrust Coefficient

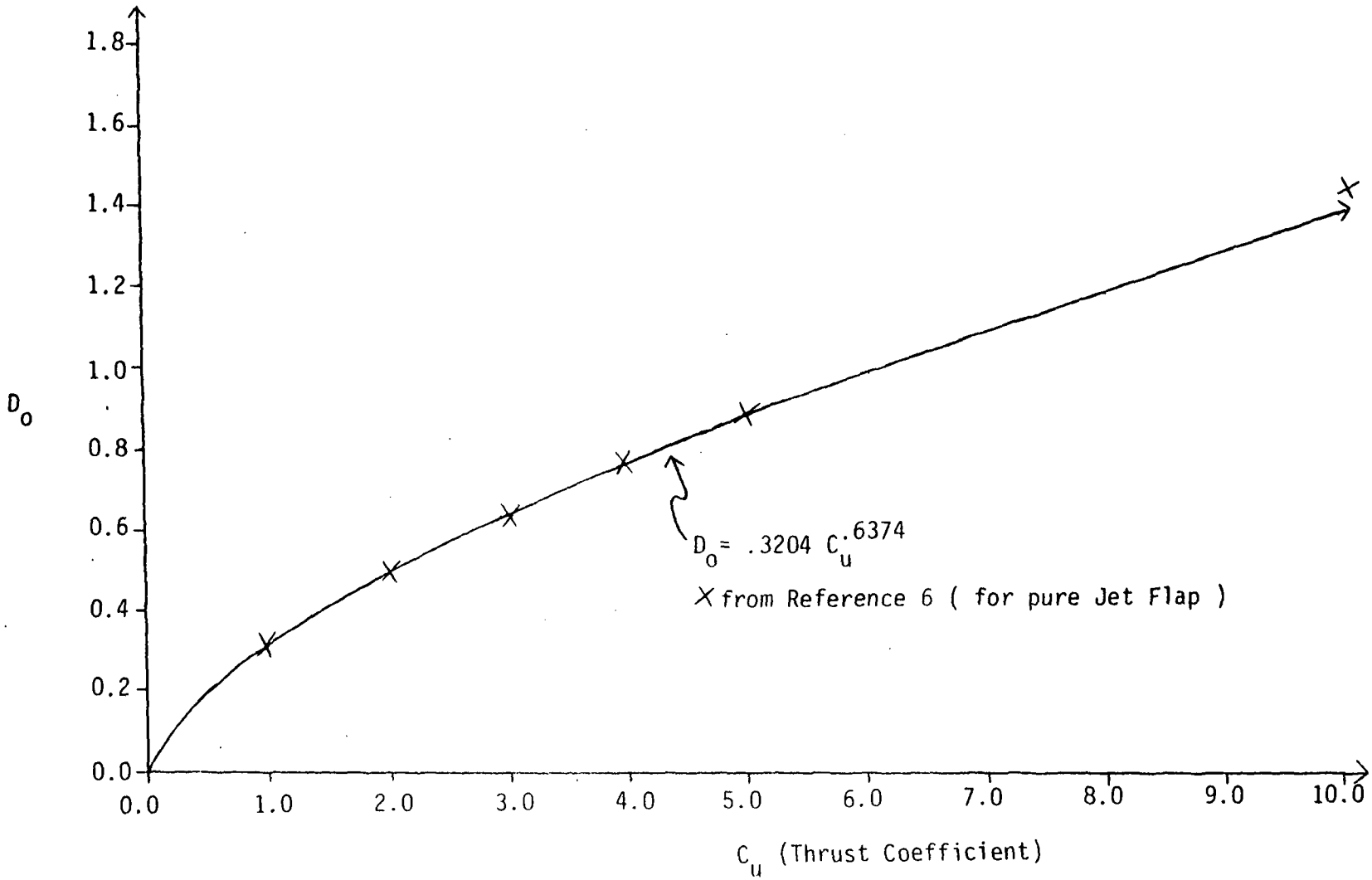

FIGURE 9- Curve of Fourier Coefficient D_o Versus Thrust Coefficient

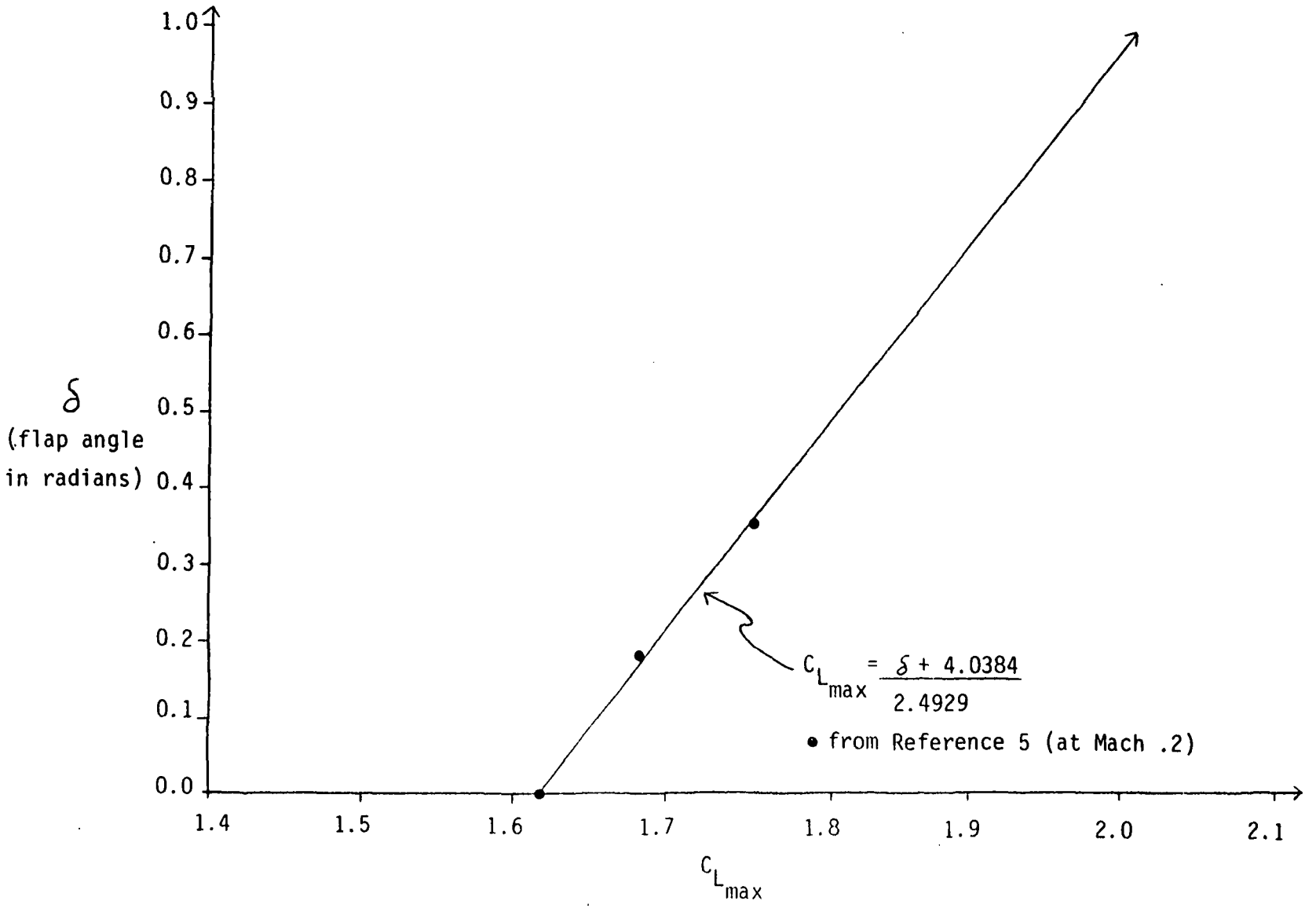

FIGURE 10- Curve Fit of Flap Angle Versus Maximum Lift Coefficient

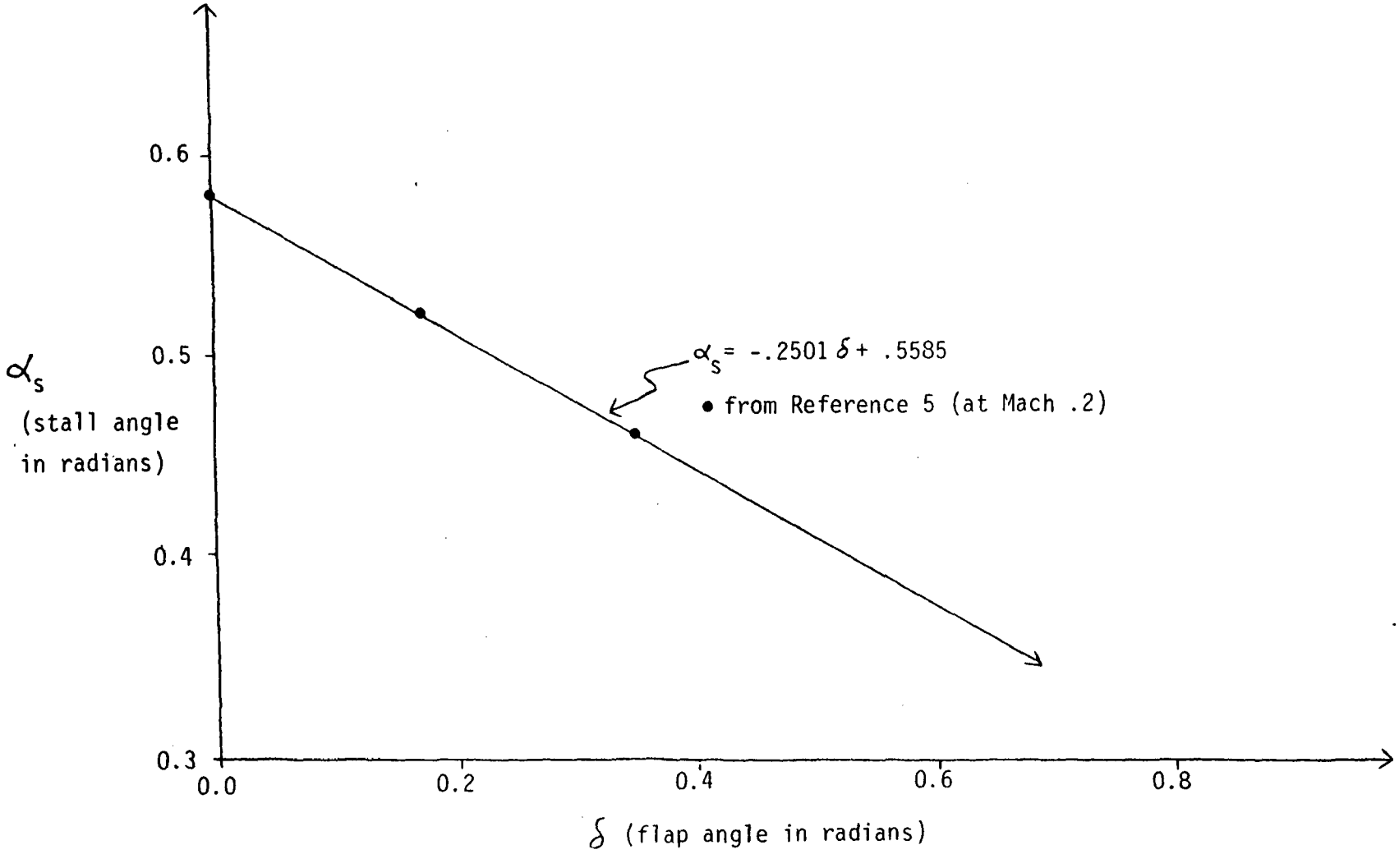

FIGURE 11- Curve Fit of Stall Angle Versus Flap Angle

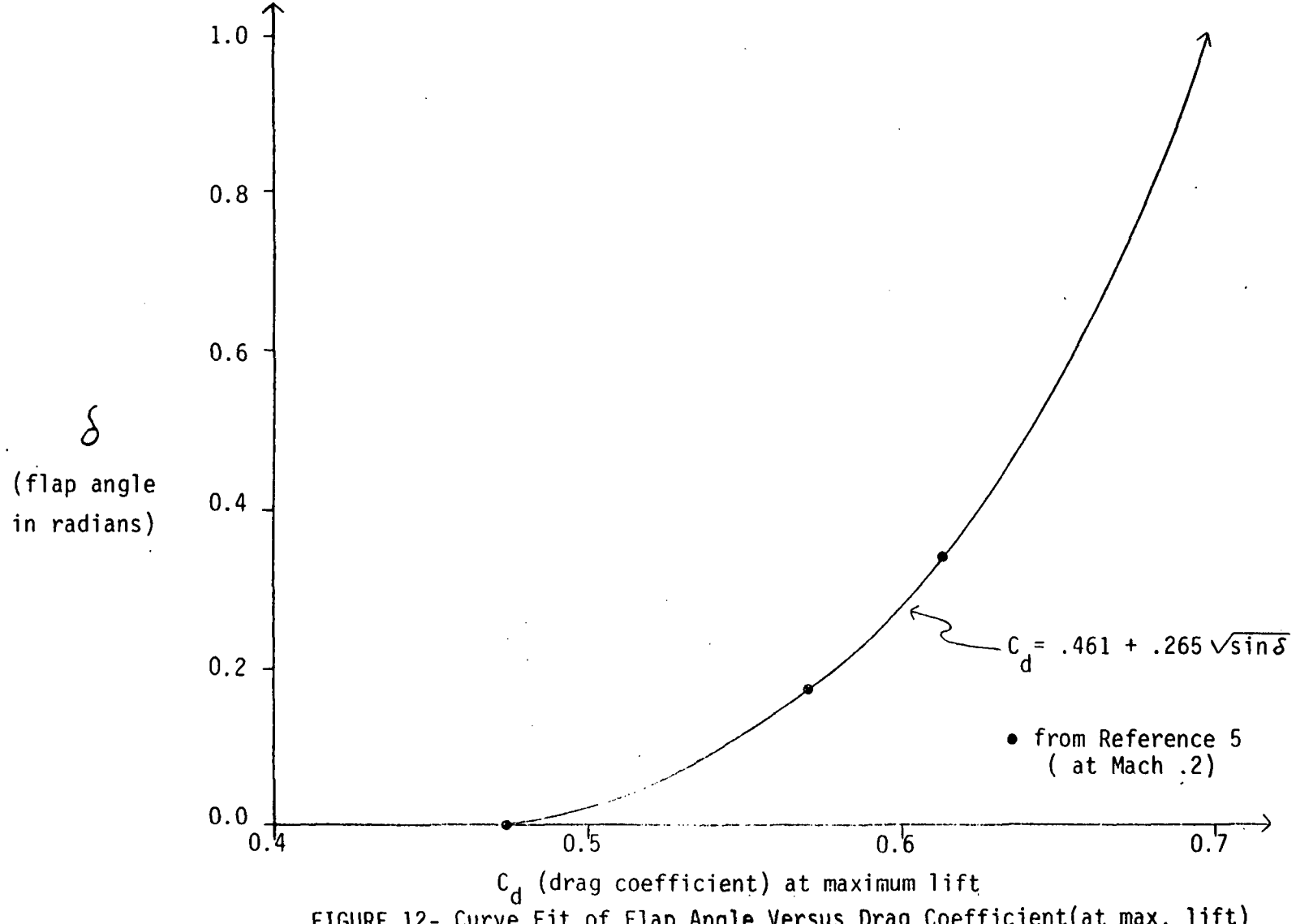

FIGURE 12- Curve Fit of Flap Angle Versus Drag Coefficient(at max. lift)

```
C*************************************************************************
C
C
C          FOR A SPECIFIC TAKEOFF VELOCITY,THIS PROGRAM CALCULATES
C             THE MAXIMUM BALANCED LIFT OF THE MODEL 279-3
C             MODIFIED TO ACCEPT A JET FLAP, THEN COMPUTES
C             THE GROUND ROLL NECCESSARY TO REACH THE
C             TAKEOFF VELOCITY.
C
C
C             VARIABLE LISTING:
C             -----------------
C               V=TAKEOFF VELOCITY
C               V1=INITIAL VELOCITY FOR ITTERATION
C               V2=FINAL VELOCITY FOR ITTERATION
C               VD=VELOCITY INCREMENT
C               VEL=VELOCITY USED FOR GROUND RUN CALC.
C               THFRNT=FRONT NOZZLE GROSS THRUST
C               THRERG=REAR NOZZLE GROSS THRUST
C               THFN=NET FRONT NOZLE THRUST
C               TOTTH=TOTAL THRUST FOR GROUND RUN CALCULATION
C               THRN=NET REAR NOZZLE THRUST
C               W=CALCULATED MAXIMUM TAKEOFF WEIGHT
C               FM=MOMENT FROM FRONT NOZZLE
C               RM=MOMENT FROM REAR NOZZLE  + JET FLAP LIFT
C               LIMIT=LOWER LIMIT ON LATERAL ACCELERATION(=a/g)
C               ACC=ACCELERATION
C               X=GROUNDRUN PER VELOCITY INTERVAL
C               D=DRAG PER VELOCITY INTERVAL
C               XT=TOTAL GROUND RUN
C               T=TIME
C               Q=DYNAMIC PRESSURE
C               VTHF=VERTICAL THRUST OF FRONT NOZZLE
C               S=WING AREA
C               RHO=ATMOSPHERIC DENSITY
C               H=STEPSIZE FOR GROUND ROLL CALCULATION
C               DIFF=DIFFERENCE BETWEEN REQUIRED & COMPUTED HOR. THRUST
C               CD=DRAG COEFFICIENT
C               D=TOTAL DRAG
C               F=NET THRUSTING FORCE(THRUST-DRAG)
C               HTH=HOR. THRUST AT TAKEOFF
C               LACCR=LATERAL ACCELERATION RATIO
```

FIGURE 13- Takeoff Performance FORTRAN Computer Program

```
C               FIRST=IDENTIFIES IF FIRST ITTERATION PER VELOCITY CALC.
C               INFLP=INFINITE LOOP COUNTER
C
C                       MOOREHOUSE VARIABLES
C               KB=PARTIAL SPAN FACTOR
C               BO=FOURIER COEFFICIENT
C               DO=FOURIER COEFFICIENT
C               DCLMXP=DELTA CL(MAX) PRIME
C               DELALF=CHANGE IN ANGLE OF ATTACK DUE TO JET FLAP
C               DCLMAX=DELTA CL(MAX)=CHANGE IN MAX CL
C               DCLJF=CHANGE IN AERODYNAMIC LIFT ( NO MOMENTUM TERM ) DUE TO
C                     JET FLAP
C               CLMAX=MAXIMUM LIFT COEFFICIENT
C               CJ=CU=THRUST COEFFICIENT
C               ALFAO=POWER-OFF STALL ANGLE OF ATTACK
C               ALFAU=POWER-ON STALL ANGLE OF ATTACK
C               DELTAR=REAR NOZZLE ANGLE(RELATIVE TO AIRCRAFT CENTERLINE)
C               DELTAF=FRONT NOZZLE ANGLE(RELATIVE TO AIRCRAFT CENTERLINE)
C
C
C
C
C*****************************************************************************
C
C
C
C
C                *DECLARATIONS*
      REAL BO,DO,DELTAR,ALFAU,ALFAO,DELALF,DCLMXP,CJ
      REAL A,B,VCMOMR,KB,V,DCLMAX,CLMAX,RHO,THFRNT,W,S
      REAL DELTAF,THRERG,DELRD,THRN,DELFD,ALFAUD,DCLJF
      REAL VTHF,TOTTH,VEL(11),D(11),H,XT,LACCR,X(11),HTH
      REAL Q,FM,RM,T,F(11),ACC,DIFF,LIMIT,CD(11)
C
      INTEGER N,L,K,I,J,P,INFLP
      LOGICAL FIRST
C               *INITIALIZATION*

      FIRST=.TRUE.
      N=0
      L=0
      K=0
```

FIGURE 13 (cont.)

```
      J=0
      P=0
      INFLP=0
      V1=60.
      V2=128.
      VD=8.
      DELTAR=1.57079
      DELTAF=1.57079
      THFRNT=24431.
      THRERC=13989.
      RHO=.002377
      V=V1
    5 Q=.5*RHO*(V**2.)
      KB=.35
      S=428.4
C
      THRN=THRERC
      CJ=THRN/(Q*S)
      THFN=THFRNT
      TOTTH=(THRN+THFN)*COS(.17453)
      VTHF=THFN
C
C
C        *CALCULATE MAX LIFT AS PER MOORHOUSE REPORT*
C
C
      BO=.185*(CJ**.833)
      DO=.3204*(CJ**.6374)
   10 N=N+1
      ALFAO=-.2501*DELTAR+.733
      A=(BO*ALFAO+DO*DELTAR)/(1+BO/2.)
      DELALF=-.5*A
      ALFAU=DELALF+ALFAO
      B=(3.+.637*CJ)/(5.+.604*SQRT(CJ)+.876*CJ)
      DCLMXP=5.5*3.14159*A*B
      VCMOMR=CJ*SIN(DELTAR+ALFAU)
      DCLMAX=KB*(DCLMXP-VCMOMR)+VCMOMR
      CLMAX=(DELTAR+4.0384)/2.4929
      IF (DELTAR .LT.0)THEN
      PRINT*,'DELTAR<0'
      GOTO 150
      ENDIF
C
C
```

FIGURE 13 (cont)

```
C       *CALCULATE MOMENTS AND BALANCE AIRPLANE*
C
C
  12    FM=(VTHF)*4.75
        RM=(DCLMAX-VCMOMR)*Q*S*3.344
     +  +6.2*THRN*SIN(DELTAR+ALFAU)-304.*6.2
        IF(FM .LT. RM)THEN
        DELRD=DELTAR*57.296
        IF(L .EQ. 0)WRITE(6,115)DELRD
        L=L+1
        DELTAR=DELTAR-.0043633
        GOTO 10
        ENDIF
C
C
C        *MAX STALL ANGLE OF ATTACK SET AT 5 DEGREES*
C
C
C
        IF (ALFAU .LT. .08727)THEN
        IF (K .EQ. 0)WRITE(6,120)
        K=K+1
        DELTAR=DELTAR-.0043633
        GOTO 10
        ENDIF
C
C
C          *CALCULATE TAKEOFF WEIGHT*
C
C
        W=(CLMAX+DCLMAX)*Q*S+VTHF
C
C
        DELRD=DELTAR*57.296
        ALFAUD=ALFAU*57.296
        DELFD=DELTAF*57.296
        DCLJF=DCLMAX-VCMOMR
        INFLP=INFLP+1
        IF(INFLP .GT. 90)GOTO 150
        WRITE (100)
        WRITE (6,110)V,DELRD,DELFD,ALFAUD,DCLJF,W
        IF(P .EQ.1)GOTO 150
C
C
```

FIGURE 13 (cont.)

```
C          *BEGIN CALCULATION OF TAKEOFF DISTANCES*
C
C
      H=V/10.
      XT=0.
      VEL(1)=0.
      DO 15 I=1,10
      J=I+1
      VEL(J)=H*I
   15 CONTINUE
C
      DIFF=0.
C
      DO 25 N=1,10
      CD(N)=.461+.265*SQRT(SIN(DELTAR))
      D(N)=CD(N)*.5*RHO*(VEL(N+1)**2.)*S
      F(N)=TOTTH-D(N)
      ACC=F(N)*32.174/W
      T=H/ACC
      X(N)=((VEL(N+1)+VEL(N))/2.)*T
      XT=XT+X(N)
   25 CONTINUE
C
C
C          *MAKE SURE A/C>.065(SUFFICIENT LONGITUDINAL ACCELERATION)*
C
C
      IF (FIRST)DELTAF=1.570796-ALFAU
      HTH=THRN*COS(DELTAR+ALFAU)-D(10)+THFN*COS(DELTAF+ALFAU)
      LIMIT=.065*W
      IF(HTH .LT. LIMIT)THEN
      DIFF=LIMIT-HTH
      DELTAF=ACOS((COS(DELTAF+ALFAU)*THFN+DIFF)/THFN)-ALFAU
      VTHF=THFN*SIN(DELTAF+ALFAU)
      W=W-(THFN-VTHF)
      WRITE(6,114)
  114 FORMAT(1H ,'DRAG TOO BIG,ROTATING F.NOZZLE BACK')
      FIRST=.FALSE.
      GOTO 12
      ENDIF
C
```

FIGURE 13 (cont.)

```
      LACCR=HTH/32.174
      DELRD=DELTAR*57.296
      DELFD=DELTAF*57.296
      WRITE(6,116)
      WRITE(6,117)XT,W,VEL(11),DELRD,DELFD,D(10),HTH
  116 FORMAT(' ',37X,'REAR',7X,'FRONT',/,2X,'TAKEOFF',16X,
     2 'TAKEOFF',6X,'NOZZLE',5X,'NOZZLE',5X,'TAKEOFF',3X,
     3 'TAKEOFF',/,2X,'DISTANCE',4X,'WEIGHT',5X,'VELOCITY',
     4 5X,'ANGLE',6X,'ANGLE',6X,'DRAG',7X,'HOR THRUST',/,
     5 2X,'(FT)',8X,'(LBF)',6X,'(FT/S)',8X,'(DEG)',6X,'(DEG)',
     6 6X,'(LBF)',7X,'(LBF)',/,2X,'--------',4X,'------',
     7 5X,'---------',5X,'------',5X,'--------',4X
     8 ,'---------',5X,'-----',/)
C
  117 FORMAT(' ',2X,F6.1,5X,F7.1,5X,F5.1,8X,F5.1,
     2 5X,F5.1,5X,F7.1,5X,F7.1,//)
C
C
C          *LOOP TO UPDATE NEW TAKEOFF VELOCITY & RECALCULATE
C              TAKEOFF DISTANCE,ETC.*
C
C
      IF(V .LT.V2)THEN
      V=V+VD
      DELTAR=1.570796
      L=0
      K=0
      FIRST=.TRUE.
      GOTO 5
      ENDIF
C
C
  100 FORMAT(' ',17X,'REAR',6X,'FRONT',/,13X,'NOZZLE',4X,
     2 'NOZZLE',4X,'STALL',/,5X,'VELOCITY',5X,'ANGLE',
     3 5X,'ANGLE',5X,'ANGLE',5X,'CLIMB',6X,'WEIGHT',/,5X,
     4 '(FT/S)',7X,'(DEG)',5X,'(DEG)',5X,'(DEG)',5X
     5 ,'CHANGE',5X,'(LBF)',/,5X,'---------',5X,
     6 '------',4X,'------',4X,'---------',5X,
     7 '------',5X,'------',/)
  110 FORMAT(' ',4X,F6.2,5X,F6.3,5X,F6.3,4X,F6.3,5X,
     2 F5.2,6X,F7.1,//)
  115 FORMAT(' ','MOMENTS ARE TOO BIG WITH DELTAR=',
     2 F4.1,3X,'DECREASING DELTAR')
  120 FORMAT(' ','ALFAU<0,DECREASING DELTAR')
  150 STOP
      END
```

FIGURE 13 (cont.)

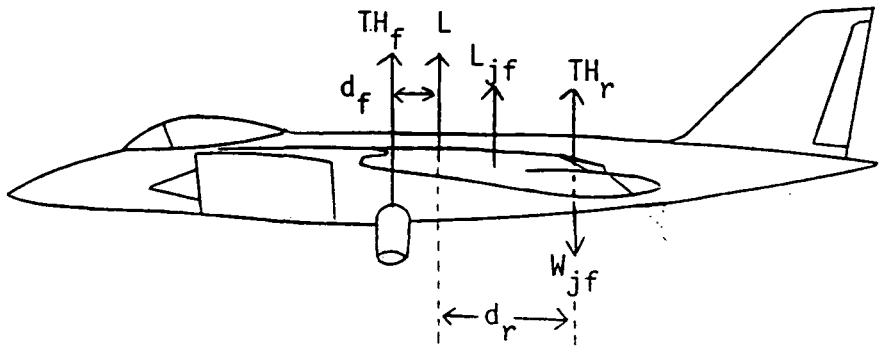

L= Lift of Wing without Jet Flap(acts at $\frac{C_{mac}}{4}$)

L_{jf} = Aerodynamic Lift Benefit of Jet Flap(acts at $\frac{C_{mac}}{2}$)

TH_f = Vertical Thrust of Front Nozzles

TH_r = Vertical Thrust of Jet Flap(acts through flap hinge)

W_{jf} = Weight of Jet Flap(acts through flap hinge)

Center of Gravity at $\frac{C_{mac}}{4}$

Moments due to Canard and Reaction Control System neglected

Moment due to vertical distance between nozzles neglected

To Balance Aircraft

Positive Pitching Moments = Negative Pitching Moments

$$TH_f * d_f + W_{jf} * d_r = L_{jf} * \frac{C_{mac}}{4} + TH_r * d_r$$

FIGURE 14

Model 279-3JF Takeoff Balancing Criteria

```
C*************************************************************************
C
C       THIS PROGRAM CALCULATES THE INSTANTANEOUS TURNING RATE AND
C          RADIUS FOR THE JET FLAPPED MODEL 279-3, AT 10,000 FT.
C          AND MACH .4
C
C            VARIABLE LISTING:
C            -----------------
C              V= VELOCITY
C              THRC=REAR NOZZLE CROSS THRUST
C              THFC=FRONT NOZZLE CROSS THRUST
C              Q=DYNAMIC PRESSURE
C              S=WING AREA
C              RHO=ATMOSPHERIC DENSITY
C              TR=TURNING RATE
C              N=LOAD FACTOR(L/W)
C              L=TOTAL LIFT(INCLUDING THRUST IN DIRECTION OF LIFT)
C              RADIUS=INSTANTANEOUS TURNING RADIUS
C              PHI=TURNING ANGLE
C              W=WEIGHT(26260 LBF)
C
C
C                    MOOREHOUSE VARIABLES
C              KB=PARTIAL SPAN FACTOR
C              BO=FOURIER COEFFICIENT
C              DO=FOURIER COEFFICIENT
C              DCLMXP=DELTA CL(MAX)-PRIME
C              DELALF=CHANGE IN ANGLE OF ATTACK DUE TO JET FLAP
C              DCLMAX=DELTA CL(MAX)= CHANGE IN MAX CL
C              DCLJF=CHANGE IN AERODYNAMIC LIFT ( NO MOMENTUM TERM ) DUE TO
C                    JET FLAP
C              CLMAX=MAXIMUM LIFT COEFFICIENT
C              CJ=CU=THRUST COEFFICIENT
C              ALFAO=POWER-OFF STALL ANGLE OF ATTACK
C              ALFAU=POWER-ON STALL ANGLE OF ATTACK
C              DELTAR=REAR NOZZLE ANGLE(RELATIVE TO AIRCRAFT CENTERLINE)
C              DELTAF=FRONT NOZZLE ANGLE(RELATIVE TO AIRCRAFT CENTERLINE)
C
C*************************************************************************
```

FIGURE 15- Instantaneous Turning Performance FORTRAN Computer Program

```
C
C
C           *DECLARATIONS*
      REAL BO,DO,DELTAR,ALFAU,ALFAO,DELALF,DCLMXP,CJ
      REAL A,B,VCMOMR,KB,V,DCLMAX,CLMAX,RHO,THFG,THRG
      REAL TR,L,N,PHI,RADIUS
      REAL DELRD
C
C           *INITIALIZATION*

      V=430.96
      DELTAR=1.57079
      THFG=21251.
      THRG=12045.
      RHO=.0017556
    5 Q=.5*RHO*(V**2.)
      KB=.35
      S=428.4
      CJ=THRG/(Q*S)
C
C           *CALCULATE MAX LIFT AS PER MOORHOUSE REPORT*
C
C

      BO=.185*(CJ**.833)
      DO=.3204*(CJ**.6374)
      ALFAO=.5236
      A=(BO*ALFAO+DO*DELTAR)/(1+BO/2.)
      DELALF=-.5*A
      ALFAU=DELALF+ALFAO
      IF ((DELTAR+ALFAU) .GT. 1.57079)THEN
        DELTAR=DELTAR-.017453
        GOTO 5
      ENDIF
      B=(3.+.637*CJ)/(5.+.604*SQRT(CJ)+.376*CJ)
      DCLMXP=5.5*3.14159*A*B
      VCMOMR=CJ*SIN(DELTAR+ALFAU)
      DCLMAX=KB*(DCLMXP-VCMOMR)
      CLMAX=1.9+DCLMAX
C
```

FIGURE 15 (cont.)

```
C
C              *NOW CALCULATE LOAD FACTOR,TURNING RATE,AND TURNING RADIUS*
C
      L=(CLMAX)*Q*S+THRC+THFG
      N=L/26260.
      TR=32.174/V*SQRT(N**2-1)*180./3.1415926
      PHI=ACOS(1.0/N)
      RADIUS=V**2/(32.174*TAN(PHI))
C
C
C
      DELRD=DELTAR*180./3.14159
      WRITE(6,100)TR,RADIUS,N,DELRD
      WRITE(6,111)RHO,V
  111 FORMAT(' ','FOR RHO =',2X,F10.9,2X,'& V= ',2X,F8.2)
      WRITE(6,222)THFG,THRC
  222 FORMAT(' ','THFG=',2X,F10.2,' & THRC=',2X,F10.2)
  100 FORMAT(' ','TURN RATE IS',2X,F5.2,/,1X,'TURN RADIUS IS',2X,F9.2
     2 /,1X, 'LOAD FACTOR IS',2X,F5.2,/'REAR NOZZEL ANGLE IS',2X,F5.2)
      PRINT*,CJ,A,B,CLMAX,L,VCHOMR
C
C
      STOP
      END
```

FIGURE 15 (cont.)

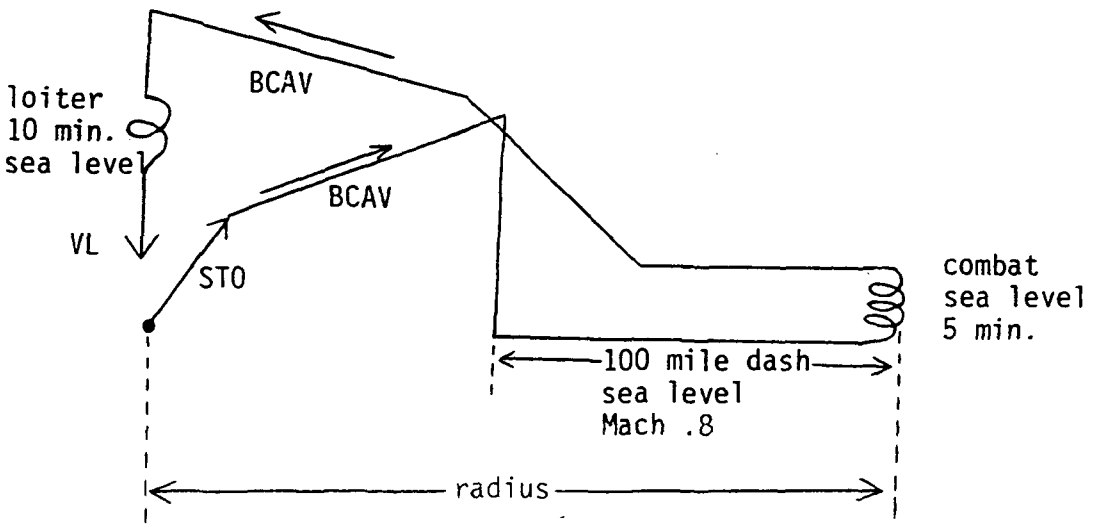

COMBAT- Drop Bombs
- Retain Missiles

5% Reserve Fuel

No Fuel, Time, or Distance Credited for Descent

BCAV= Best Cruise Altitude and Velocity

VL= Vertical Landing

STO= Short Takeoff (250 ft. maximum)

FIGURE 16

Model 279-3 and 279-3JF Interdiction Comparison Mission Profile

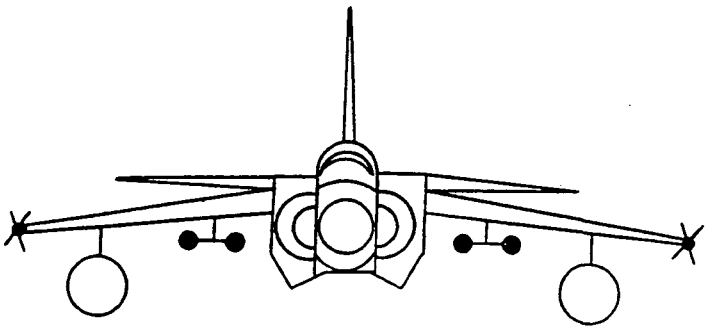

4 MK 82 Bombs

2 X 600 Gallon Fuel Tanks

2 Short Range Air to Air Missiles (SRAAM)

GROSS TAKEOFF WEIGHT

42,000 lbf.

TAKEOFF DISTANCE

250 ft.

MISSION RADIUS

152 miles

FIGURE 17

Model 279-3 Comparison Mission
Configuration and Performance

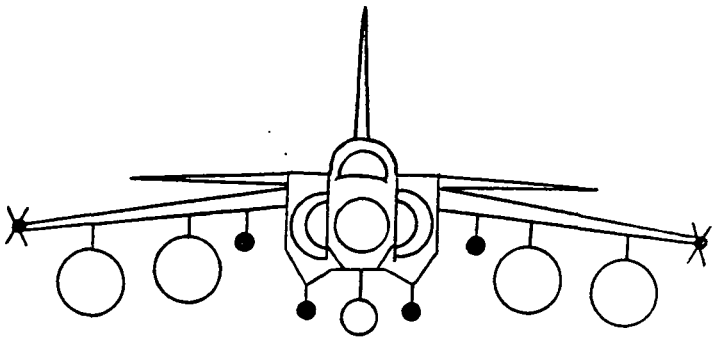

4 MK 82 Bombs

4 X 600 Gallon + 1 X 120 Gallon Fuel Tanks

2 Short Range Air to Air Missiles (SRAAM)

GROSS TAKEOFF WEIGHT
(including weight of Jet Flap)

53,925 lbf.

TAKEOFF DISTANCE

210 ft.

MISSION RADIUS

564 miles

FIGURE 18

Model 279-3JF Comparison Mission (with added fuel)
Configuration and Performance

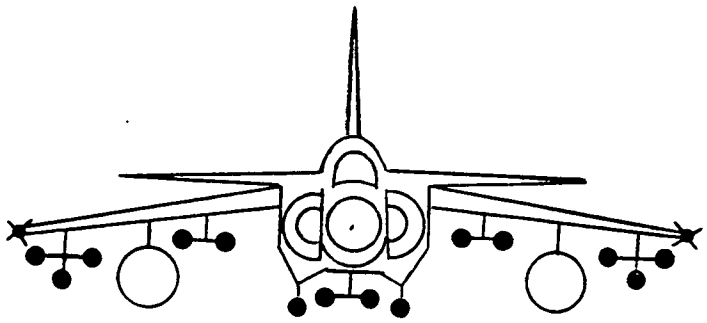

14 MK 82 Bombs

2 X 600 Gallon Fuel Tanks

2 Short Range Air to Air Missiles (SRAAM)

GROSS TAKEOFF WEIGHT
(including weight of Jet Flap)

54,000 lbf.

TAKEOFF DISTANCE

211 ft.

MISSION RADIUS

174 miles

FIGURE 19

Model 279-3JF Comparison Mission (with added bombs)
Configuration and Performance

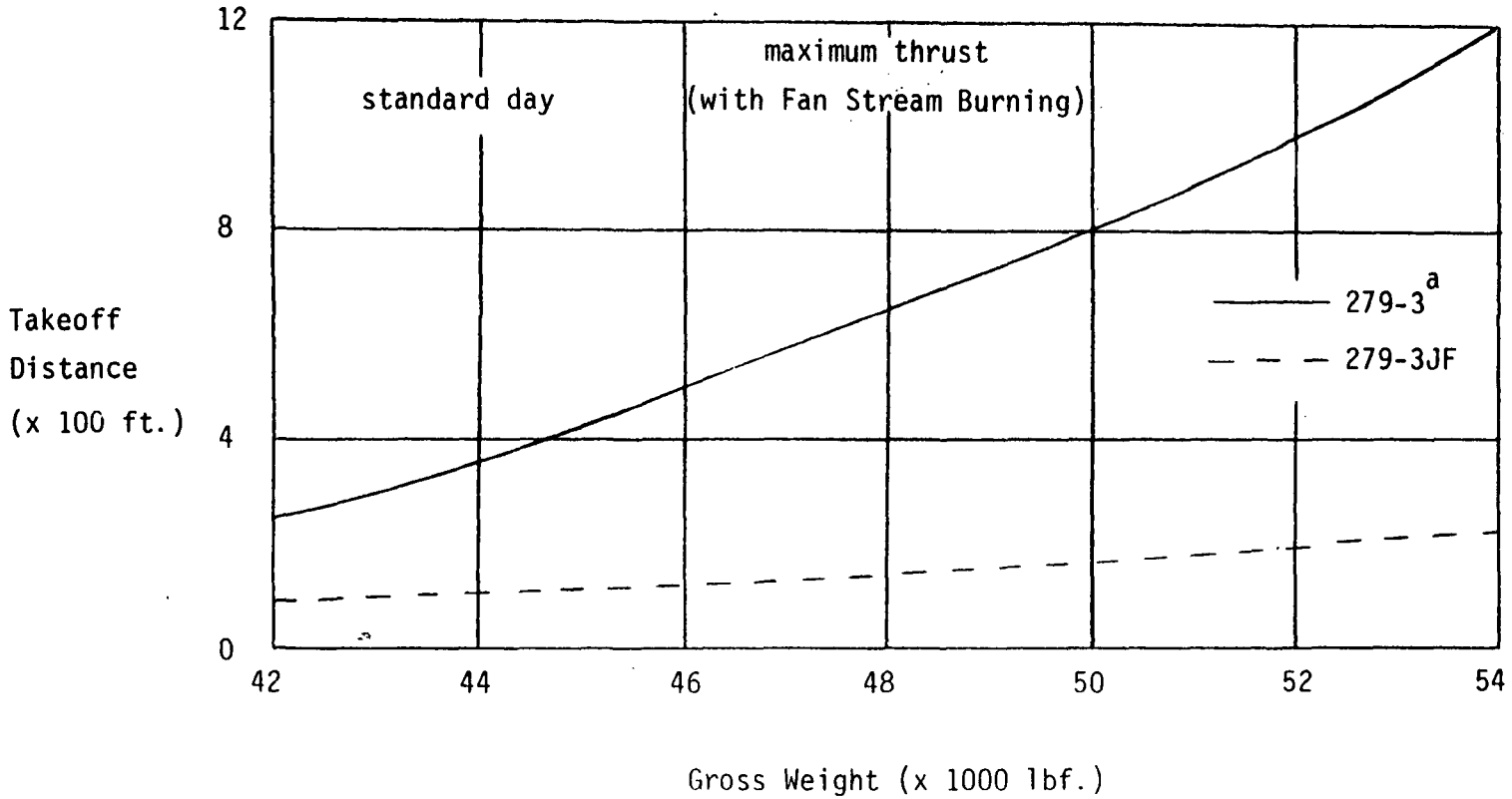

FIGURE 20- Model 279-3 and 279-3JF Short Takeoff Capability

[a]From Reference 5

TABLE 2

MODEL 279-3JF DETAILED TAKEOFF CONDITIONS

(output from Program of Figure 13)

Weight (lbf.)	Takeoff Distance (ft)	Lift off Velocity (ft/s)	Rear[a] Nozzle Angle (deg)	Front[a] Nozzle Angle (deg.)	Stall Angle (deg.)	Aerodynamic Jet Flap C_L increase
40573.3	61.1	60	41.3	85.0	5.020	1.38
41265.9	66.5	62	42.5	84.9	5.094	1.41
42002.0	72.2	64	44.0	85.0	5.016	1.43
43435.4	84.6	68	46.5	84.9	5.093	1.47
44166.9	91.3	70	47.8	85.0	5.112	1.49
44908.6	98.3	72	49.0	84.9	5.118	1.50
45660.8	105.8	74	50.3	84.9	5.113	1.51
46423.7	113.6	76	51.5	84.9	5.096	1.53
47197.5	121.9	78	52.8	84.9	5.068	1.54
48737.7	139.7	82	55	84.9	5.106	1.55
49545.1	149.3	84	56.3	85.0	5.047	1.56
50321.6	159.3	86	57.3	84.9	5.102	1.56
51152.2	169.9	88	58.5	85.0	5.025	1.57
52750.7	192.3	92	60.5	83.3	5.084	1.57
53556.1	204.3	94	61.5	82.3	5.099	1.58
54036.1	211.2	95.1	62.3	81.8	5.001	1.58
55587.0	236.6	99	64	79.8	5.100	1.58
56406.2	250.5	101	65	78.8	5.086	1.58

TABLE 2 (continued)

Weight (lbf.)	Takeoff Distance (ft)	Lift off Velocity (ft/s)	Rear[a] Nozzle Angle (deg)	Front[a] Nozzle Angle (deg.)	Stall Angle (deg.)	Aerodynamic Jet Flap C_L increase
56817.3	257.6	102	65.5	78.3	5.076	1.58
57642.2	272.4	104	66.5	77.3	5.051	1.58
58470.9	287.8	106	67.5	76.2	5.018	1.57
59258.8	303.6	108	68.3	75.2	5.090	1.57
60094.7	320.3	110	69.3	74.2	5.044	1.57
60399.6	334.6	112	67.3	73.0	6.301	1.51
60781.8	349.7	114	65.8	71.8	7.317	1.46
61157.5	365.3	116	64.3	70.7	8.312	1.41
61575.4	381.7	118	63.0	69.6	9.181	1.37
61988.8	398.5	120	61.8	68.5	10.032	1.32
62397.4	415.7	122	60.5	67.4	10.866	1.28
62801.3	433.5	124	59.3	66.4	11.685	1.24
63200.3	451.7	126	58.0	65.4	12.488	1.21
64466.0	469.5	128	57.0	64.4	13.172	1.17

[a]Relative to aircraft centerline

TABLE 3

MODEL 279-3 and 279-3JF

INSTANTANEOUS TURNING PERFORMANCE

Maximum Thrust with Thrust Vectoring

Aircraft	Sea Level Mach .3		10,000 ft. Mach .4		20,000 ft. Mach .5		30,000 ft. Mach .6	
	Turning Rate $\left(\frac{\text{Degrees}}{\text{sec}}\right)$	Turning Radius (ft)	Turning Rate $\left(\frac{\text{Degrees}}{\text{sec}}\right)$	Turning Radius (ft)	Turning Rate $\left(\frac{\text{Degrees}}{\text{sec}}\right)$	Turning Radius (ft)	Turning Rate $\left(\frac{\text{Degrees}}{\text{sec}}\right)$	Turning Radius (ft)
279-3[a]	28	641	19.5	1264	17.0	1704	13.0	2627
279-3JF	38.0	505	31.4	786	24.9	1194	18.8	1813

[a]Reference 5

TABLE 4

INSTANTANEOUS TURNING RATES OF 279-3JF

AND OTHER AMERICAN AND SOVIET FIGHTERS

AIRCRAFT	Turn Rate $\left(\frac{\text{Degrees}}{\text{sec}}\right)$ at 15,000 ft. Mach. 5
Model 279-3JF	30.0
Mig-21[a]	13.4
F5-E[a]	11.4
Mig-23[a]	8.6
F-4[a]	7.8
F-15[a]	16.5
F-16[a]	15.6

[a]Reference 9

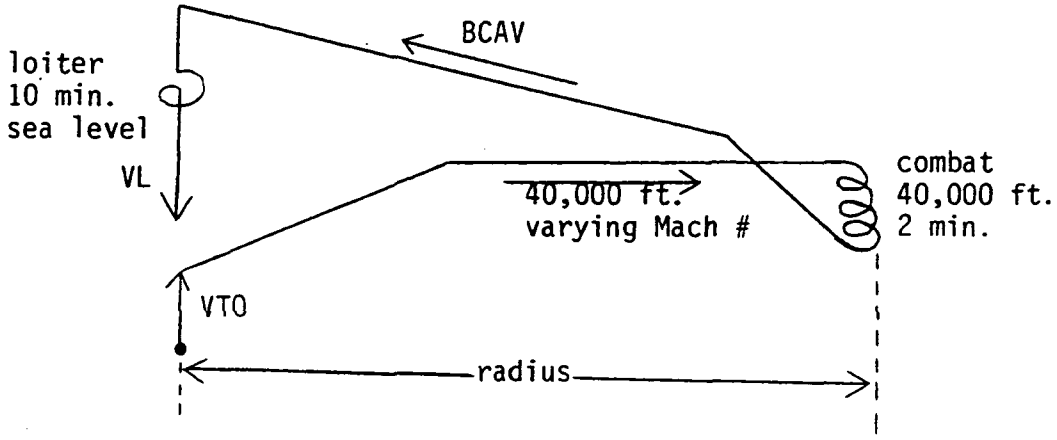

Armament- 2 Advanced Medium Range Air to Air Missiles (AMRAAM)

- 2 Short Range Air to Air Missiles (SRAAM)

Combat- Retain all Missiles

No Fuel, Time, or Distance Credited for Descent

BCAV= Best Cruise Altitude and Velocity

VL= Vertical Landing

VTO= Vertical Takeoff

5% Reserve Fuel

FIGURE 21

Model 279-3 Deck Launched Intercept Mission Profile

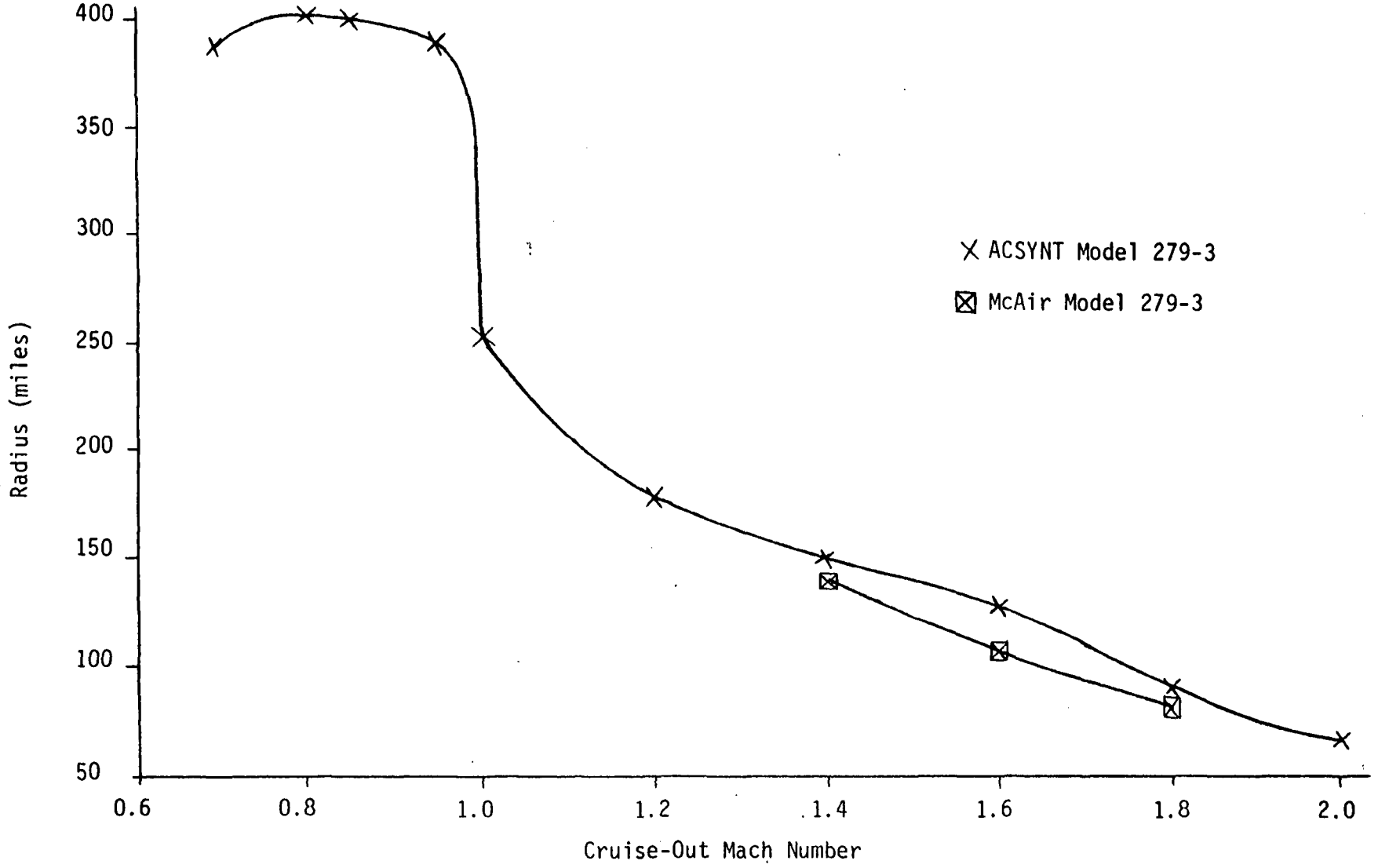

FIGURE 22

Model 279-3 Deck Launched Intercept Mission Performance

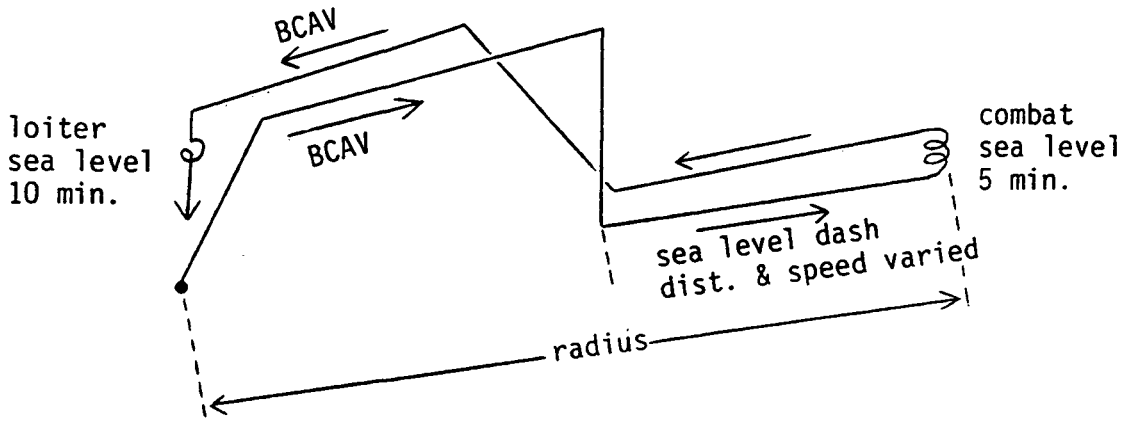

Armament- 14 MK 82 Bombs
- 2 Short Range Air to Air Missiles (SRAAM)

Combat- Drop Bombs
- Missiles Retained
- 2 X 600 Gallon Fuel Tanks Dropped When Empty

No Distance, Time, or Fuel Credited for Descent

BCAV= Best Cruise Altitude and Velocity

5% Reserve Fuel

FIGURE 23

Model 279-3 Interdiction Mission Profile

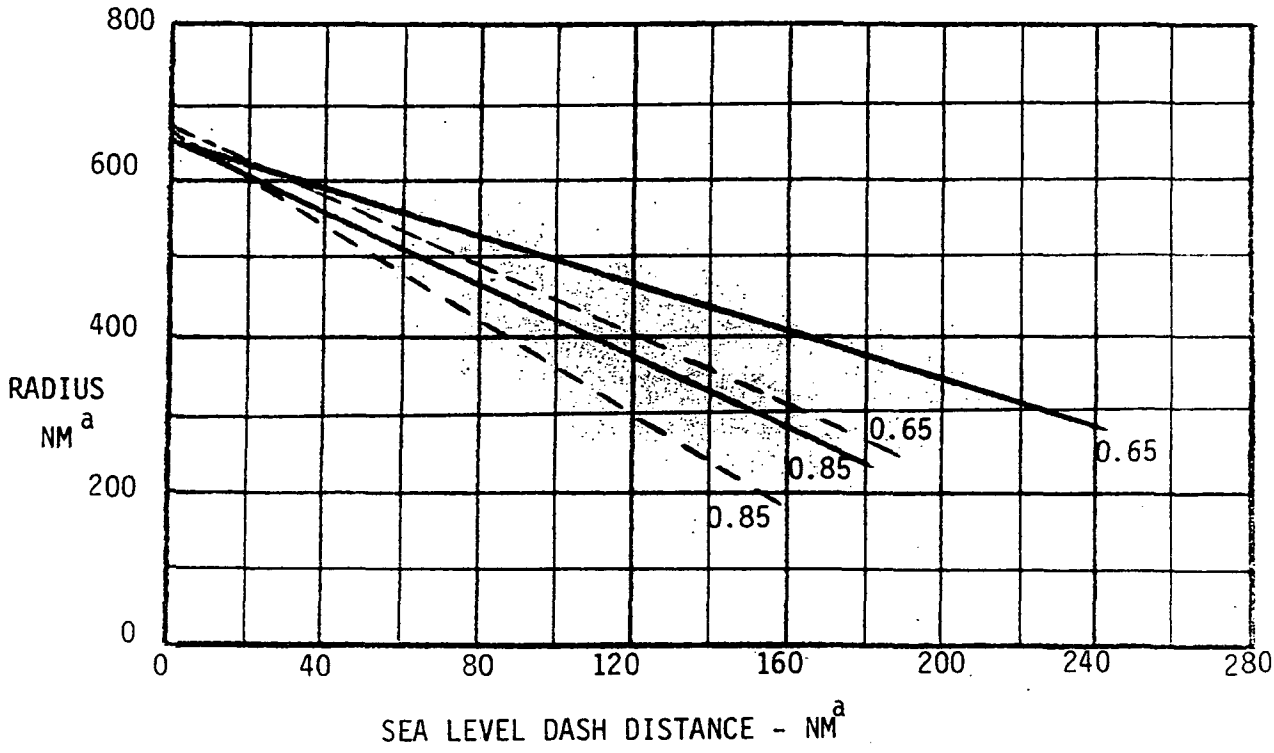

FIGURE 24

Model 279-3 Interdiction Mission Performance

APPENDIX B

THE MODELED 279-3

APPENDIX B

THE MODELED 279-3

Modeling the 279-3 was accomplished by using NASA's "Aircraft Synthesis" (ACSYNT) FORTRAN program, which is briefly explained in the text. The computer modeled aircraft is an important design tool. Data can be obtained for the 279-3 on any desired mission, and is not limited to that supplied by the contractor. This is important because the 250 ft. takeoff distance interdiction mission chosen to compare the 279-3 and the 279-3JF was not studied by the contractor. Once the effect of the jet flap is determined, the modeled 279-3 can be altered by merely changing program input variables, to model the 279-3JF. Thus, the modeling technique made it possible to compare the mission performance of the two aircraft.

Even though the mission studied in this report was not studied by the contractor, it is still important to compare the ACSYNT modeled 279-3 to the McAir modeled 279-3. This ensures that the model is correct, and calibrates the contractor's performance estimates. For this purpose, the ACSYNT model was examined on two missions studied by McAir. The first mission is the deck launched intercept mission given in Figure 21. The mission performance is given in Figure 22. Note that the ACSYNT model produced a wider range of data than that provided by the contractor, which was useful in evaluating the 279-3. The slight departure in the ranges between the two aircraft at Mach 1.6 is due to the slight inaccuracies of the ACSYNT engine model. Modeling

the engine over the entire Mach number and altitude envelope of the aircraft is a difficult task. In order to obtain the highest degree of accuracy in the more typical high altitude and high subsonic flight regimes, accuracy was sacrificed in supersonic (above Mach 1.5) and very low altitude (below 10,000 ft.) flight. It should be noted that engine data used by McAir was proprietary in nature, and was not available. The ACSYNT engine was modeled using data from state of the art engine prediction codes and represents an excellent approximation. Considering this, the correlation between the two curves is very good. It is interesting to note, in Figure 22, the rapid drop in range, with cruise out Mach numbers of around one. This is because the engine must produce more thrust to overcome wave drag, increasing fuel consumption.

The second mission used to compare the two models of the 279-3 is the interdiction mission described in Figure 23. The performance of the two models are plotted in Figure 24. Notice that as the sea level dash distance increases, the two models deviate in mission radius. This indicates that the difference in performance is due to the low level inaccuracies of the ACSYNT engine model. In fact, with no low level dash distance, the two aircraft ranges agree within 26 miles, out of a total mission radius of 650 miles. This is a difference of only four percent and demonstrates ACSYNT's high degree of accuracy.

Since the ACSYNT model compares favorably to the McAir Model 279-3, it can be modified to predict the performance of the jet flapped 279-3JF. Any slight errors that exist in the ACSYNT model

279-3 do not affect its comparison to the 279-3JF, because these errors are common to both aircraft.

REFERENCES

1. Spence, D.A., "The Lift Coefficient of a Thin, Jet-Flapped Wing," Proceedings of the Royal Society of London, Vol. A238, 1956, pp. 46-68.

2. Wilson, R.E., "Summary of Two-Dimensional Tunnel Tests of a Wing Employing Pressure Slots and Flaps," United Aircraft Corporation, Research Laboratories Report R-278-d, 1944.

3. Bevilaqua, P.M., Schum, E.F., and Woan, C.J., "Progress Towards a Theory of Jet Flap Thrust Recovery," AIAA report 83-0079, January 1983.

4. Sedgwick, T.A., (Lockheed California Co.) "Investigation of Augmented Deflector Exhaust Nozzles Installed in Tactical Aircraft," AFFDL TR75-42, May 1975.

5. Hess, J.R., and Bear, R.L., "Study of Aerodynamic Technology for Single Cruise Engine V/STOL Fighter/Attack Aircraft," NASA CR-166269, March 1982.

6. Moorhouse, D.J., "Predicting the Maximum Lift of Jet-Flapped Wings," Conference on V/STOL Aerodynamics, Delft, Netherlands, April 1974.

7. Moorhouse, D.J., "A Practical Look at the Stall and High Lift Operation of Externally Blown Flap STOL Transport Configurations," Conference on Fluid Dynamics of Aircraft Stalling, Lisbon, Portugal, April 1972.

8. Engine Data received from Charles L. Zola, Aerospace Engineer for National Aeronautics and Space Administration, Lewis Research Center, Cleveland, OH.

9. Robinson, C.A., Jr., "Mig-21 Playing Defensive Role," Aviation Week and Space Technology, December 21, 1981, pp. 34-37.